THE CIRCUMFERENTIAL PROPAGATION PROCESS FOR THE MAGNETIZATION OF TAPE WOUND CORES

GEORGE W. DAVIS

THE CIRCUMFERENTIAL PROPAGATION PROCESS FOR THE MAGNETIZATION OF TAPE WOUND CORES

* * * * *

George W. Davis

THE CIRCUMFERENTIAL PROPAGATION PROCESS FOR THE MAGNETIZATION OF TAPE WOUND CORES

By

George W. Davis
//
Lieutenant, United States Navy

Submitted in partial fulfillment of
the requirements for the degree of

MASTER OF SCIENCE
IN
ELECTRICAL ENGINEERING

United States Naval Postgraduate School
Monterey, California

1 9 6 3

THE CIRCUMFERENTIAL PROPAGATION PROCESS FOR THE MAGNETIZATION OF TAPE WOUND CORES

By

George W. Davis

This work is accepted as fulfilling
the thesis requirements for the degree of

MASTER OF SCIENCE

IN

ELECTRICAL ENGINEERING

from the

United States Naval Postgraduate School

ABSTRACT

A theory is developed describing the process by which a signal induced at one point on a ferromagnetic toroidal core propagates to other locations about the core. Both qualitative and quantitative arguments are presented to support this description. An experiment is discussed which tests the proposed theory. A complete analysis of the results of this experiment is made and includes a quantitative comparison of the measured results with those predicted by the theory. In as much as this comparison shows excellent agreement between the experimental results and theoretical predictions, the proposed theory appears to explain quite adequately the circumferential propagation process in magnetic cores.

The author wishes to express his appreciation for the assistance and encouragement given by Professor Charles H. Rothauge, and Mr. Raymond B. Yarbrough of the U. S. Naval Postgraduate School and of Mr. Bernard M. Loth of the Lawrence Radiation Laboratory.

TABLE OF CONTENTS

LIST OF ILLUSTRATIONS

1. Introduction

There is a relatively large volume of information in today's literature explaining the processes believed to occur in the normal magnetization or "switching" in tape wound ferro-magnetic cores. Since most of the interest has been centered around the magnetization in small cores with uniformly distributed windings, little information is available on the process this author chooses to call "the circumferential propagation process"; that is, the process by which a signal induced at one point on a magnetic core migrates to other points about the core circumference. Such a process is not normally of consequence when the core has a uniform distribution of windings since the signal is induced at all points about the core circumference. When large diameter cores are to be used in very fast pulse circuits, such a process becomes quite important. To illustrate this point, assume that a core of diameter 25 cm is excited at one point by a single turn primary. If the signal traveled on or in the core at the speed of light, it would arrive at a secondary winding placed diametrically opposite the primary after a 2.5 ns delay. One would guess that the actual velocity of signal propagation, that is the circumferential propagation velocity, would be somewhat less than the speed of light. If the velocity were an order of magnitude less, a delay of 25 ns would result. A 25 ns delay is somewhat longer than rise times encountered in modern high power pulse circuits. Even though these delays are significant in such circuits, this author could find no published reference explaining or even theorizing on the process by which a signal might propagate from the region of an exciting winding to

other locations about a magnetic core. It appears that further improvement in high power pulse circuits might well depend on an understanding of this process. Therefore, it is the intent of this thesis to develop a theory, based on presently accepted ferro-magnetic concepts (such as those presented in reference 1) to explain the process of circumferential propagation in ferro-magnetic torroidal cores.

2. A Theory on the Circumferential Propagation Process

2.1 Development of the Theory

Under the action of an applied field, flux reversal in magnetic tape begins with the formation of domains of reversed magnetization. In the normal polycrystaline magnetic tape, these domains form at crystal imperfection such as voids, inclusions, etc. on or near the tape surface; then grow inward into the tape. The formation of these domains, the so called nucleation process, requires a certain minimum applied field and hence energy. Once this nucleus of reversed magnetization is formed, it expands by domain wall motion at a rate dependent on the magnitude of the applied field. As these domain walls grow, colliding and consolidating with those from neighboring nucleation sites, the region of reversed flux continues to enlarge. This process will continue until either all of the flux in the tape has been reversed or the applied field is reduced below some minimum coercive force. (1)

While the above constitutes only a very brief description of the magnetization process, two concepts essential to the development of the subject theory are introduced. First, the nucleation process will take place whenever a suitably oriented applied field at a nucleation site exceeds some minimum magnitude. Second, provided the applied field is maintained above some other minimum value*, the domain wall will grow into the tape from the nucleation sites. Hence, there exist only two modes by which a signal induced at one point on the circumference of a magnetic toroid can propagate to some other point on the core. Once applied, the signal must either travel internally by means of domain wall motion or

*The applied field necessary to move a domain wall is less than that required to form the wall. See reference (1).

over the surface in the form of an E-M wave originating flux reversals at surface nucleation sites wherever they occur in the path of travel of the wave.

Domain wall motion constitutes a linear transfer of energy in the direction of this wall movement. Since this energy is supplied by the magnetic forcing field, the direction of transfer must be that of the Poynting vector associated with this field. Therefore domain wall motion is in a direction perpendicular to the applied magnetic field. This domain wall motion is always accompanied by eddy currents which circulate in accordance with Lenz's law in such a manner as to oppose the applied field. These currents increase with increase in wall velocity, thus creating a requirement for higher applied fields to maintain the initial wall motion. A signal, then, could not be propagated in the circumferential direction by this mode if the applied field were always parallel to the core lamenations. Certainly the leading edge of the signal wave has a component of its Poynting vector in the direction of the lamenations (or else no energy would ever transfer in this direction) and hence it is possible for domain growth to occur in such a direction. However, this growth is severely damped by the eddy current effect and its rate of propagation is many orders of magnitude less than that of the E-M signal wave over the surface of the tape.

Finally, the propagation velocity of a domain wall is directly related to the applied field. Hence, if the induced signal were propagated in this manner, the propagation velocity would be dependent upon the magnitude of this field. (2) That this is not the case will be shown experimentally.

From the above, it must be concluded that the signal applied to a

core is propagated from the point of application to the various points about the core by an electromagnetic wave. The signal radiates from the exciting winding and becomes evident in the core whenever it reaches a nucleation site with a suitably oriented component of its magnetic vector greater than the nucleation force required by the site. This is the manner in which the signal must make its circumferential progress. Since the E-M propagation velocity is independent of its amplitude, the signal applied to a toroidal core will likewise be independent of signal magnitude. Those factors which affect the time of transmission of the E-M wave from the exciting winding to outlying points on the core will also affect the time of signal transmission to the various points about the core. These effects have been investigated experimentally and the results are included in chapter 4.

2.2 The Propagation Process(for an Ideal Impulse Signal)

To illustrate the above theory graphically, consider the radiation from a single current carrying conductor as shown in figure 2-1.

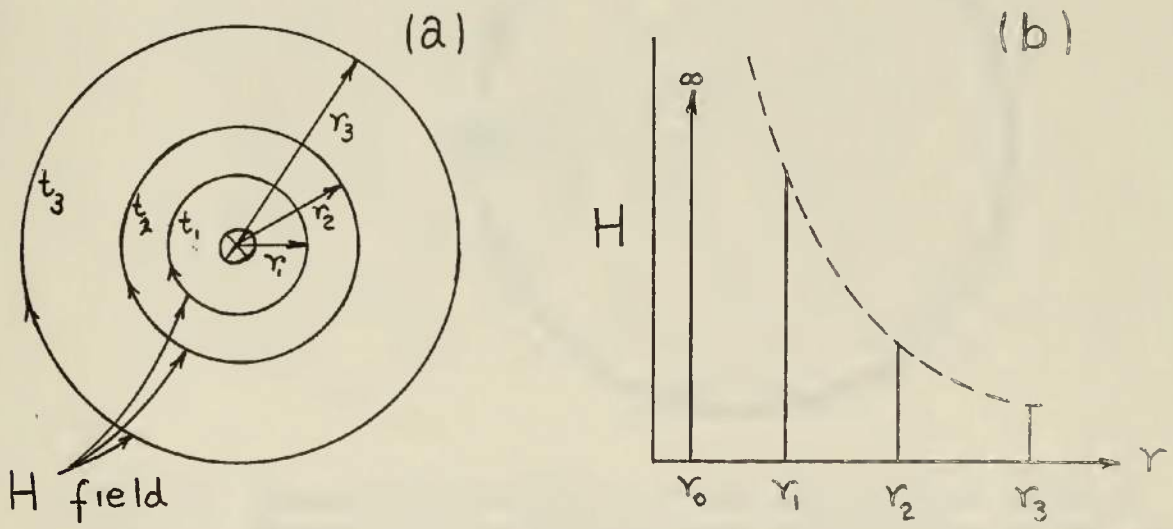

Fig. 2-1(a) Cylindrical Radiation Pattern for Impulse of Current in a single Conductor (b) Decay in Magnetic Field Intensity as a Function of Distance of Wave Travel.

If a unit impulse of current is applied to the wire, a cylindrical pulse of magnetic field propagates radially outward at the speed of light. (3) The magnitude of this pulse field decreases in amplitude as the inverse of its radial distance of travel, as predicted by Ampere's law. This magnitude decay is illustrated in Figure 2-1(b). This attenuation can be thought of in terms of a thinning out of the energy radiated in any one segment of the cylindrical field. Once this energy has been committed to a particular direction of travel it remains so directed as long as it is in the same medium.* Hence the energy density becomes less at the more remote points in space.

These ideas can now be applied in the analysis of magnetization in a large diameter magnetic ring as shown schematically in Figure 2-2 below. When an impulse of current flows in the exciting winding, a radiation pattern similar to that described above results. The characteristic of

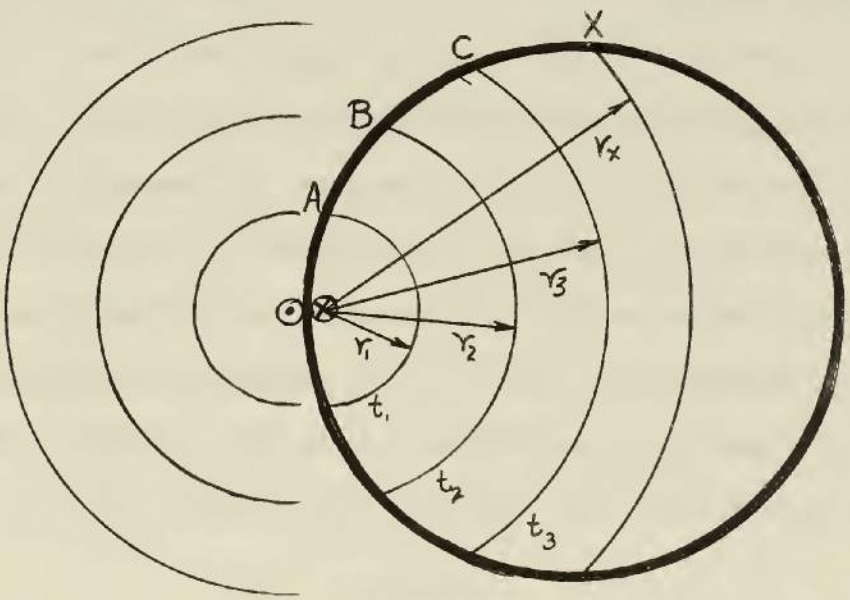

Fig. 2-2 Schematic Representation of the Magnetic Field Radiation Pattern Within a Thin Ring Magnetic Core. The Pattern is Produced by an Assumed Impulse of Current Through the Single Turn Exciting Winding.

*The direction of energy transfer will be altered when the E-M wave strikes the core.

this process that is of most interest in this discussion is the time required for the applied signal to reach points A, B, C, etc. about the core. The relationship between these time increments and the arc distance of the points A, B, C, etc. from the exciting winding will yield the apparent circumferential propagation velocity. This apparent velocity can be examined in the light of the proposed theory as follows. By trigonometric manipulations as shown in Figure 2-3, we can obtain the arc lengths O A, O B, O C, etc. as functions of time elapsed between application of the impulse and the arrival of the impulse signal at any point on the core.

$$ARC = d\alpha \qquad (2\text{-}1)$$

$$\sin \alpha = \frac{ct}{d} \qquad (2\text{-}2)$$

$$\text{or } \alpha = \sin^{-1} \frac{ct}{d}$$

d = diameter of core

α = half angle subtended by an arc with respect to the toroid center

c = velocity of light

By solving the above equations graphically with an assumed core diameter of 40 cm, the plot of arc length against elapsed time shown in Figure 2-4 was obtained. The slope at any particular point on this graph represents the apparent circumferential propagation velocity for the corresponding location on the core. Obviously this slope, that is velocity, is not constant even though the energy associated with the signal travels over the chord lengths at a constant rate. In fact, this apparent point velocity must approach infinity as r approaches the diameter of the core. This can be shown by substituting $\sin^{-1} \frac{ct}{d}$ for α in (2-1). Then:

$$\text{Arc} = d \sin^{-1} \frac{ct}{d}$$

differentiating arc length with respect to time to obtain apparent propagation velocity:

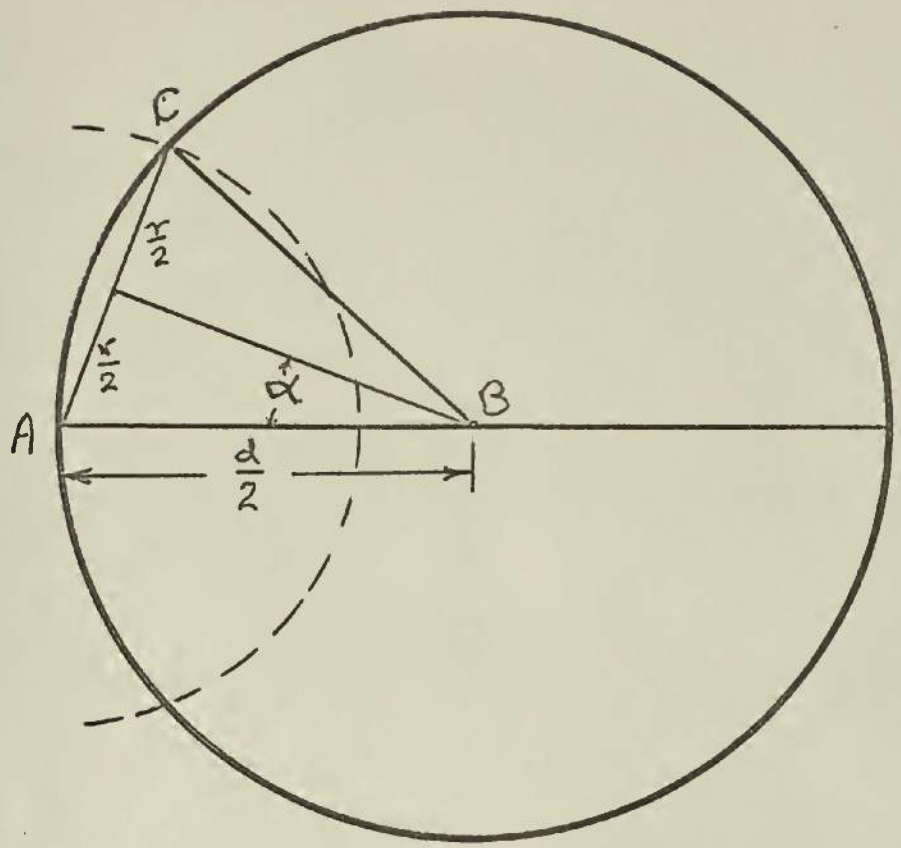

ARC $AC = \left(\frac{d}{2}\right)(2\alpha) = d\alpha$

SIN $\alpha = \frac{r/2}{d/2} = \frac{r}{d}$

$\therefore$ ARC $AC = d \sin^{-1} \frac{r}{d}$ but $r = ct$

OR $= d \sin^{-1} \frac{ct}{d}$

FIG 2-3: DERIVATION OF COPE TRIGONOMETRY

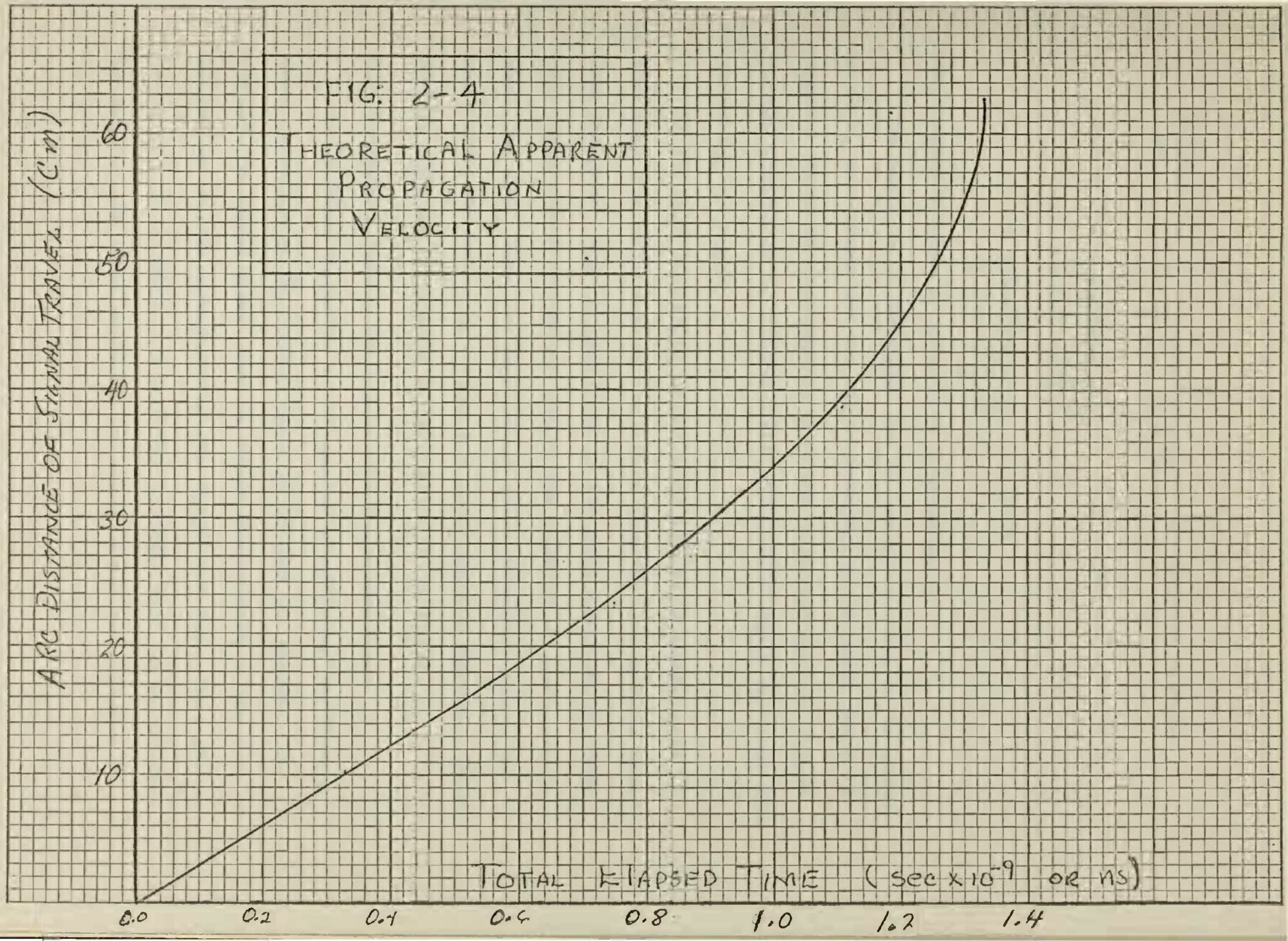
FIG. 2-4
THEORETICAL APPARENT PROPAGATION VELOCITY
ARC DISTANCE OF SIGNAL TRAVEL (CM)
60
50
40
30
20
10
0.0
0.2
0.4
0.6
0.8
1.0
1.2
1.4
TOTAL ELAPSED TIME (SEC X 10⁻⁹ OR NS)

$$\frac{d(Arc)}{dt} = \left[\frac{\frac{c}{d}}{\sqrt{1-\left(\frac{ct}{d}\right)^2}}\right] \quad d = \text{Apparent Velocity}$$

$$\text{App. Vel.} = \frac{c}{\sqrt{1-\left(\frac{ct}{d}\right)^2}} \qquad \text{but } ct = r$$

$$= \frac{c}{\sqrt{1-\left(\frac{r}{d}\right)^2}} \qquad (2\text{-}3)$$

This expression goes to infinity as r approaches d.

The amplitude of the signal (or the energy) arriving at the points A, B, C, etc. around the core varies inversely as the chord length of travel. Using the trigonometric relations introduced earlier, Figure 2-5 was constructed to illustrate this decrease of signal amplitude with increasing arc length.

In the above discussion, second order effects or signal noise resulting from reflections of the H field from the tape surfaces have been neglected. This is justifiable in the first approximation since they cannot effect the arrival time of the radiation at remote points about the core. Also, the magnitude of these reflections should be small since the reflecting surface is a lossy magnetic material. Nonetheless, they may be apparent as oscillation in the signal.

2.3 Propagation Process for Signals with Finite Rise Times

In the above discussion a unit impulse of sufficient amplitude to cause nucleation at the furthest point on the core was assumed. In reality, the signal cannot show the abrupt discontinuity of the unit impulse but must be accompanied by some finite rise time. This alters the results of the above in a small but important way. As was pointed out earlier, the signal amplitude (or energy level) must exceed a

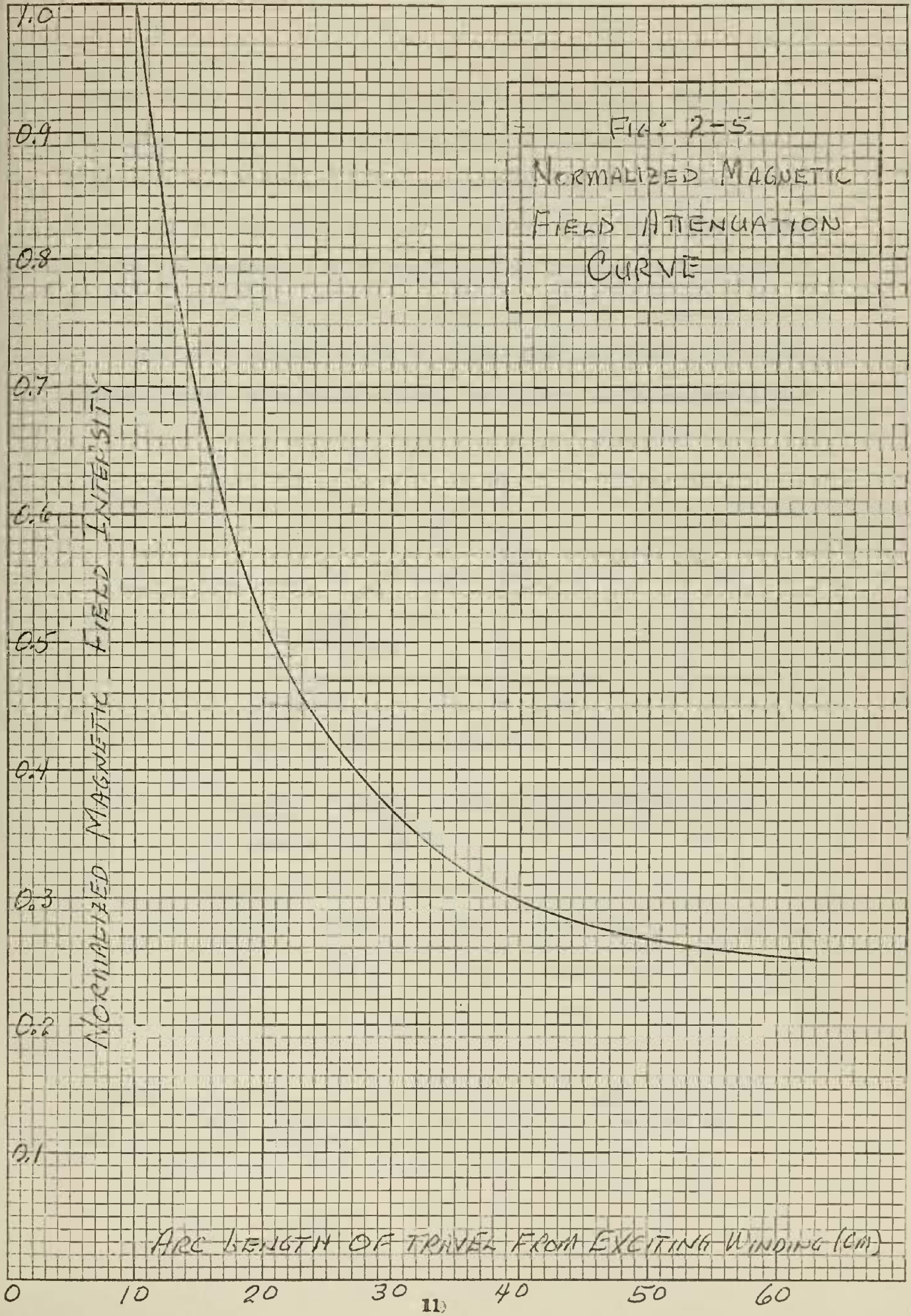

FIG. 2-5
NORMALIZED MAGNETIC FIELD ATTENUATION CURVE

certain minimum level before nucleation can take place. Hence, when the finite rise time of a realistic pulse is encountered, a certain delay will result while this pulse increases from zero to the minimum nucleation requirement for each point on the core. This delay is amplified by the decrease in pulse magnitude with increase in radial travel. To illustrate these two points, consider Figure 2-6. A ramp of current* is assumed to be applied to the exciting winding to produce the magnetic intensity pulse shown in the figure. This pulse can be expressed as a

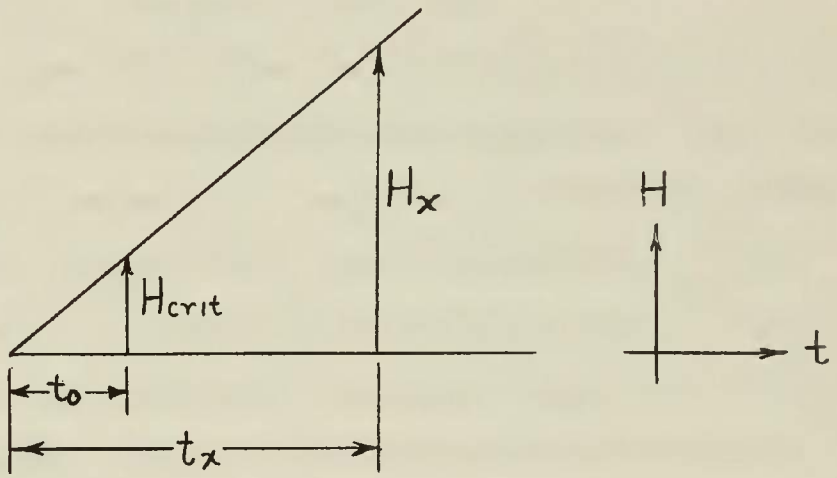

Fig. 2-6 The Ramp of Magnetic Field Intensity Resulting from a Ramp Current Function Showing H Critical and Hx as a Function of Time.

function of time in the following manner:

$$H = \frac{Kt}{l} = \frac{Kt}{2\pi r} \qquad (2\text{-}4)$$

Where K is the slope of the applied ramp of current in the units of amp-turn per second.

*As was the case with an impulse, a true ramp of current cannot be realized. However, the ramp is closer to reality than the impulse and serves well to illustrate the pertinent points.

If H crit is defined as the minimum magnetic intensity level which must exist at some point X on the core in order to produce nucleation, then the magnitude of this critical field at the exciting winding must have been, (from Equation 2-4)

$$H \text{ crit} = \frac{Kt}{2\pi r_x}$$

Where r_x is the chord distance from the exciting winding to point X on the core.

Solving for t:

$$t = t_x = \frac{2\pi r_x}{K} H \text{ crit} \quad (2\text{-}5)$$

Thus, the time t_x must expire after the application of the ramp current function before a field of sufficient initial magnitude to cause nucleation at some point X on the core is radiated from the exciting winding. An additional time, defined as Δt, must elapse while this H field travels the distance r_x to the nucleation sites at point X on the core. Again referring to the trigonometric relations of Figure 2-3, a relationship can be developed between core arc length and the total elapsed time from application of the ramp to nucleation at points on the core.

$$\text{arc} = d\alpha \text{ and } \sin\alpha = \frac{r}{d} = \frac{c\Delta t}{d}$$

$$r_x = Kt_x \text{ and } T_{total} = t_x + \Delta t$$

By assuming a value of K' and using r as the independent parameter, a graph of arc length as a function of total elapsed time can be constructed. The slope of this plot will represent the apparent circumferential propagation velocity for the ratio of signal slope to coercive force, K'.* For the sake of concreteness, a value of K' = 3.33 $\frac{cm}{ns}$ is assumed. For artitrary value of t_x and Δt, and hence T total, arc length can be calculated. A plot of values so obtained is shown in Figure 2-7.

*The derivation of numerical values for K' will be discussed in Chapter IV.

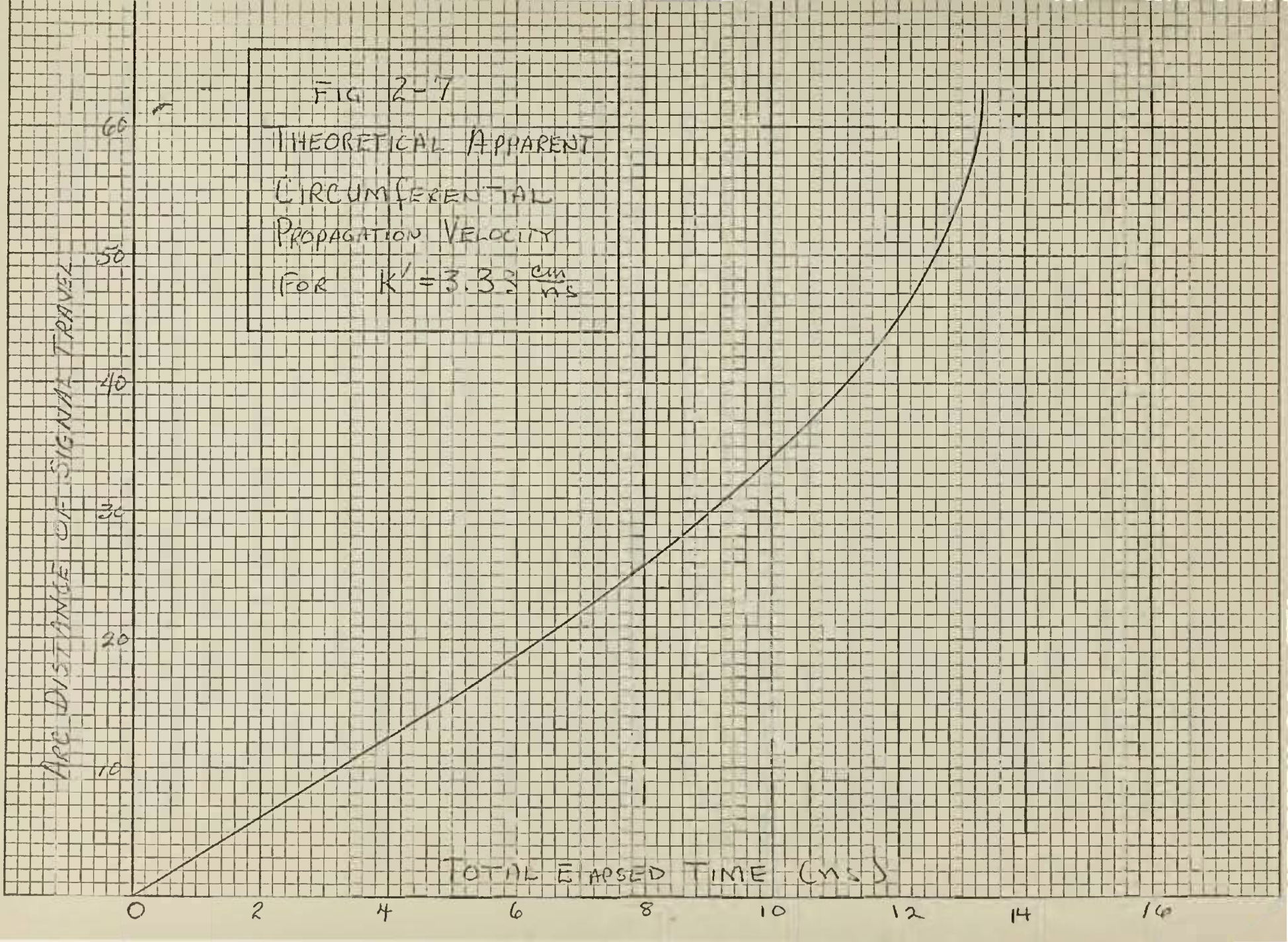
FIG 2-7
THEORETICAL APPARENT
CIRCUMFERENTIAL
PROPAGATION VELOCITY
FOR K' = 3.33 cm/ns
ARC DISTANCE OF SIGNAL TRAVEL
60
50
40
30
20
10
TOTAL ELAPSED TIME (ns)
0
2
4
6
8
10
12
14
16

The relatively long delay in the arrival of the signal at points about the core is obvious from this graph. Comparison with Figure 2-4 shows the total time required for an impulse signal to reach the point on the core diametrically opposite the exciting winding is only 1.3 ns while in the case of the ramp pulse just considered, the time required was over 13 ns. This large difference in time is clearly the result of the slope on the ramp pulse.

At this point, it is appropriate to bring together the various ideas presented and to sketch a single picture of the circumferential propagation process. The proposed theory suggests that all signal transmissions from the exciting winding to other points on the core takes place by means of an E-M wave propagating across the inner core diameter at the velocity of light. However, the intensity of this wave attenuates at a rate inversely proportional to the distance of travel from the source. If consideration is restricted to signal pulses having finite rise times,* then it can be shown that this attenuation becomes a major determinant of the apparent propagation velocity. Recall that domains of reversed magnetization are formed by the nucleation process providing that the magnetic field intensity at the nucleation site exceeds some minimum or threshold magnitude. Therefore, the signal level at the exciting winding must exceed this minimum nucleation field by the appropriate attenuation factor if it is to cause flux reversal at some remote point on the core. Since the signals being considered have a finite rise time, a delay will result while the signal reaches this "remote nucleation level" (that is, an intensity level which includes both the minimum nucleation field and the attenuation factor). This delay will increase with the distance from the

*Any physically realizable MMF pulse will have a finite rise time.

exciting winding and will thus give an apparent retardation to the propagation velocity. This is readily seen by comparing Figure 2-7 with Figure 2-4. Figure 2-4 illustrates the time required for a pulse with zero rise time to reach various points about the core. Figure 2-7 illustrates the time required for a pulse with a certain finite rise time to deliver the minimum nucleating field to the various points about the core. In the former illustration, a time of 1.3 ns is required for the signal to reach a point diametrically opposite the exciting winding while in the latter case, 13 ns are required. The difference, 11.7 ns, is identically the time required for the ramp excitation to reach the "remote nucleation level." As far as the core is concerned, it took 11.7 ns longer for the ramp pulse to reach the remote point in question than it did for the pulse with a zero rise time. Therefore the apparent signal velocity of the ramp pulse is less than that of the impulse.

A general verification of the proposed theory by experiment will be considered next. An analysis of these experimental results (Chapter IV) will further illustrate the effect of finite rise time on apparent propagation velocity.

3. Experimental Verification of the Circumferential Propagation Process

3.1 Purpose

This experiment was designed to measure the circumferential propagation velocity defined in Chapter I and to observe the effect of variations in pulse amplitude and rise time on this velocity. A comparison of these measurements with those predicted by Chapter II will be made in Chapter IV.

3.2 Procedure

The general procedure used to measure the signal velocity was to induce a fast rising step of current in an exciting winding located at one point on a magnetic core and then measure the time required for this signal to become apparent at other points about the core.

3.3 Equipment Setup

To carry out this procedure, a thin ring of 1 mil Ni-Fe tape with a ring cross section of one-half square centimeter and a mean magnetic path of 127 cm was wound with a three turn primary and six (6) single turn secondaries (or pickups) spaced about the core as shown in Figure 3-1. A reference winding, designated G, was placed inside the primary. A 2 megawatt pulser capable of delivering a 20 KV square pulse with a 15 ns rise time was used to deliver the signal to the primary. A non inductive resistance R was placed in series with the pulser to give it a current

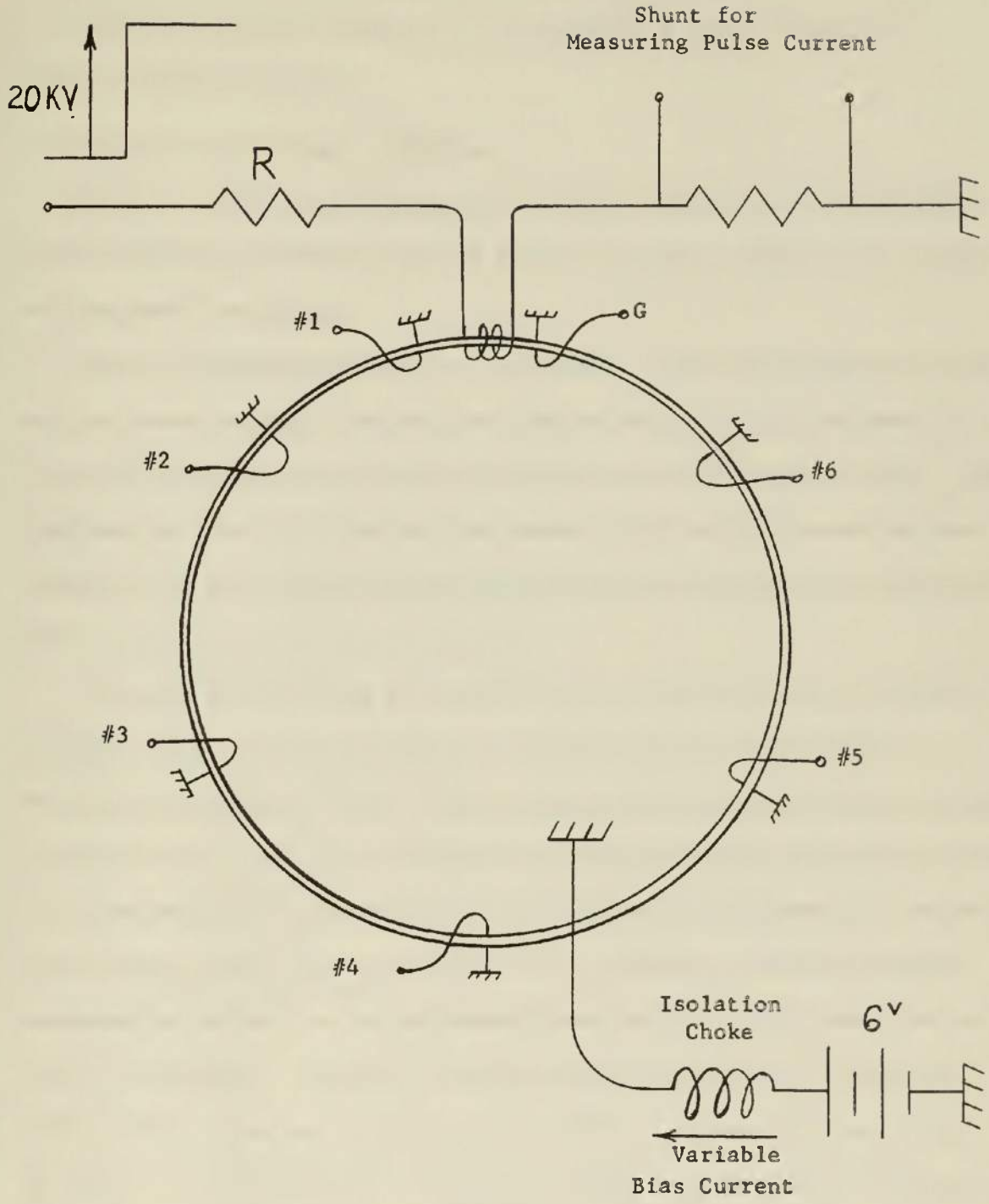

Fig. 3-1 Equipment Arrangement for Measuring the Circumferential Propagation Velocity

drive capability. The magnitude of the applied current was changed both by varying the applied voltage and by changing R while holding the applied voltage at 20 KV.

3.4 Velocity Measurement Techniques

Various methods for measuring the signal velocity were considered. The two methods used were selected because of their simplicity, reliability and reasonable accuracy.

The first method was a photo technique - consisting simply of presenting the output signals from the six pick up windings on a tektronix's 517 oscilloscope using a common time base for the horizontal sweep. When displayed on a multiply exposed photograph, the time difference between signals could be measured and compared with the known relative positions of the pick ups to obtain the velocity.

A second method using a tektonix's 576 oscilloscope with dual beam, sampling, plug in units presented an even more attractive method of obtaining the necessary data. Here, the signal from the reference winding* was presented on the "A" trace with the pickup signals being presented one at a time on the "B" trace. The two signals were simultaneously presented on the scope face as shown in Figure 3-2. The time difference between corresponding points on the reference trace and the pickup trace was recorded for each pickup. The points chosen were typically the time from 50% of the peak voltage on the "A" trace to 50% of the peak voltage on the "B" trace. A Tektronix's RS 1 digital readout unit was used to automatically

*It was found necessary to use the signal from the reference winding as the common time base for all time measurements. This eliminates the problems of accounting for time delays which might result from differences in the "A" and "B" channel probe leads. Also, since pulse comparison is the method used to determine the time delay, it is necessary that the pulses be of similar shape.

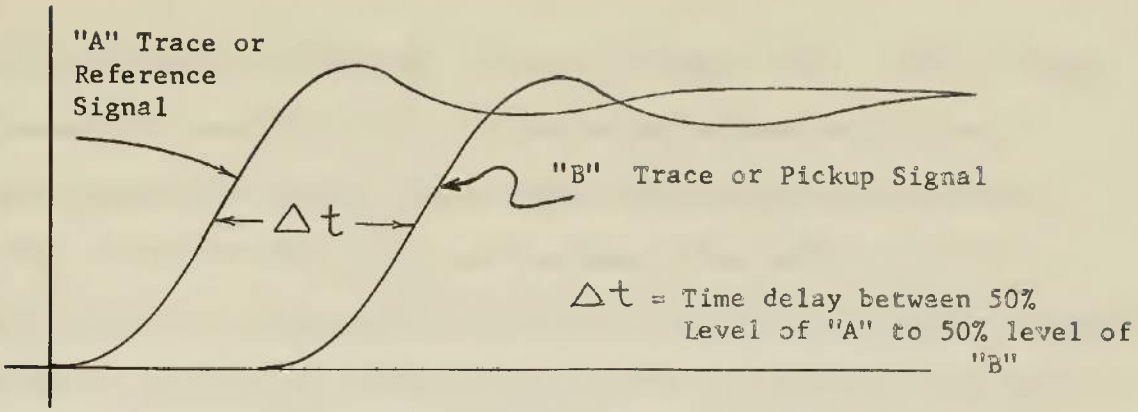

Fig. 3-2 Oscilloscope Presentation of Signal Pulses

read the time difference between the selected points. A plot of the relative positions of the pickups against the time differences so measured readily yields velocity.

3.5 Variation of Pulse Rise Time

In order to observe the effect variations in pulse rise time have on the apparent propagation velocity, the circuit of Figure 3-1 was altered to produce pulses with rise times of 45 ns, 55 ns, and 75 ns. To accomplish this, small valued (that is, 1 to 5 ohm) wire wound resistors were placed in series with the non inductive resistor, R, of the original circuit. This technique satisfactorily produced the desired variations without significantly altering the final pulse amplitude.

3.6 Attenuation Measurement

An effort was made to determine the attenuation of the signal at the various points on the core. These measurements consisted of recording the peak magnitude of the first voltage spike appearing on the pickup signal. Under most circumstances, the spike was quite evident and little room for doubt remained as to what relative point was being measured.

3.7 Summary of Experimental Results

The above procedures were carried out by successively pulsing the

core with MMF steps of 225, 168, 117, and 50 ampere turns. The rise time was maintained constant at 30 ns. Time delays between the "A" trace reference signal and the "B" trace pickup signal were recorded for the 20%, 50%, and 80% levels of the peak voltages. The position of the pickups on the core were plotted as functions of these time delays. Graphs 1 through 7 of Appendix I show these plots. The rise time for the 225 a-t pulse was altered successively to rise times of 45 ns, 55 ns, and 75 ns. Graph #8 is a plot of the apparent propagation velocity for these various rise times. Finally, pulse amplitudes at the various pickups were measured for each of the MMF pulses listed above. These are plotted in Graph #9. Graph #10 is a normalization of the data from Graph #9.

4. Analysis of Experimental Results

In an analysis of the results of the experiment described in Chapter III, the proposed theory will be examined in two respects. First, the results will be used to support the theoretical argument that the circumferential propagation of a signal by means of domain wall motion is not reasonable. Second, the results will be shown to be explainable in terms of signal transmission by means of the E-M wave as discussed in Chapter II.

It was pointed out earlier that any signal propagated by domain wall motion would travel at a velocity several orders of magnitude below that of light (2). Examination of the experimental data presented graphically in Appendix I shows the lowest value of apparent propagation velocity to be $0.294 \times 10^{10} \frac{cm}{sec.}$ This is only one order of magnitude below the velocity of light, $3.0 \times 10^{10} \frac{cm}{sec}$. Furthermore, the slope of these plots continuously increases as the distance of signal travel grows and eventually approaches infinity at the furthest point from the exciting winding. Since domain wall motion constitutes a transfer of energy, its velocity cannot exceed that of light, let alone approach infinity. Finally, there is no appreciable change in the apparent circumferential velocity with variations in the applied field which is in contradiction to the known behavior of domain wall motion. (3) In view of these experimental facts, it is evident that the apparent circumferential propagation velocity cannot be explained by domain wall motion.

To show how well the proposed theory predicts the actual experimental results, a comparison of the theoretical propagation curve of Figure 2-7 is presented in Figure 4-1 with one of the plots of experimental data. There is excellent agreement between these two curves. Not only do the

experimental points fall close alongside the predicted curve, but also the plot of the experimental data shows the increase in slope with increase in arc distance of signal travel as predicted by the proposed theory. To strengthen these arguments a detailed analysis of the experimental results will now be made in the light of the concepts presented in Chapter II.

Figure 4-1 shows a predicted curve constructed from measurable geometric parameters and a somewhat mythical parameter K'. There can be no debating of the core geometry as it is real and measurable. However, an inspection of the definition of K',

$$K' = \frac{K}{2\pi H_{critical}}$$

reveals room for considerable disagreement. H critical is the minimum coercive force necessary to cause nucleation. The value of Hc from the static hysteresis loop for Ni-Fe is approximately .1 oersted or about .085 $\frac{a\text{-}t}{cm}$. However, since a constant current bias was used to reset the core, the reset H field must be overcome before any "suitably oriented" magnetic field can affect the core. Furthermore, the bias current for each of the different levels of excitation was altered so as to just insure complete reset of the core between pulses. For example, for the 225 a-t steps a bias field of approximately 25 a-t was used while for the 117 a-t step, the bias field was reduced to 10 a-t. Therefore, the H critical appearing in the definition of K' must be computed as that amount of the applied ramp of magnetic field necessary to overcome the bias field plus the nucleation value of the magnetic field. Thus, for a 25 a-t bias, the magnetic field intensity at the tape surface would be

$$H_{reset} = \frac{NI}{l} = \frac{25 \text{ a-t}}{\text{core circumference}} = \frac{25 \text{ a-t}}{125 \text{ cm}} = .2 \frac{a\text{-}t}{cm}$$

(FIG A-1)
COMPARISON of PREDICTED PROPAGATION CURVE (Solid Line) WITH EXPERIMENTAL Results (SHOWN IN Circled Dots)

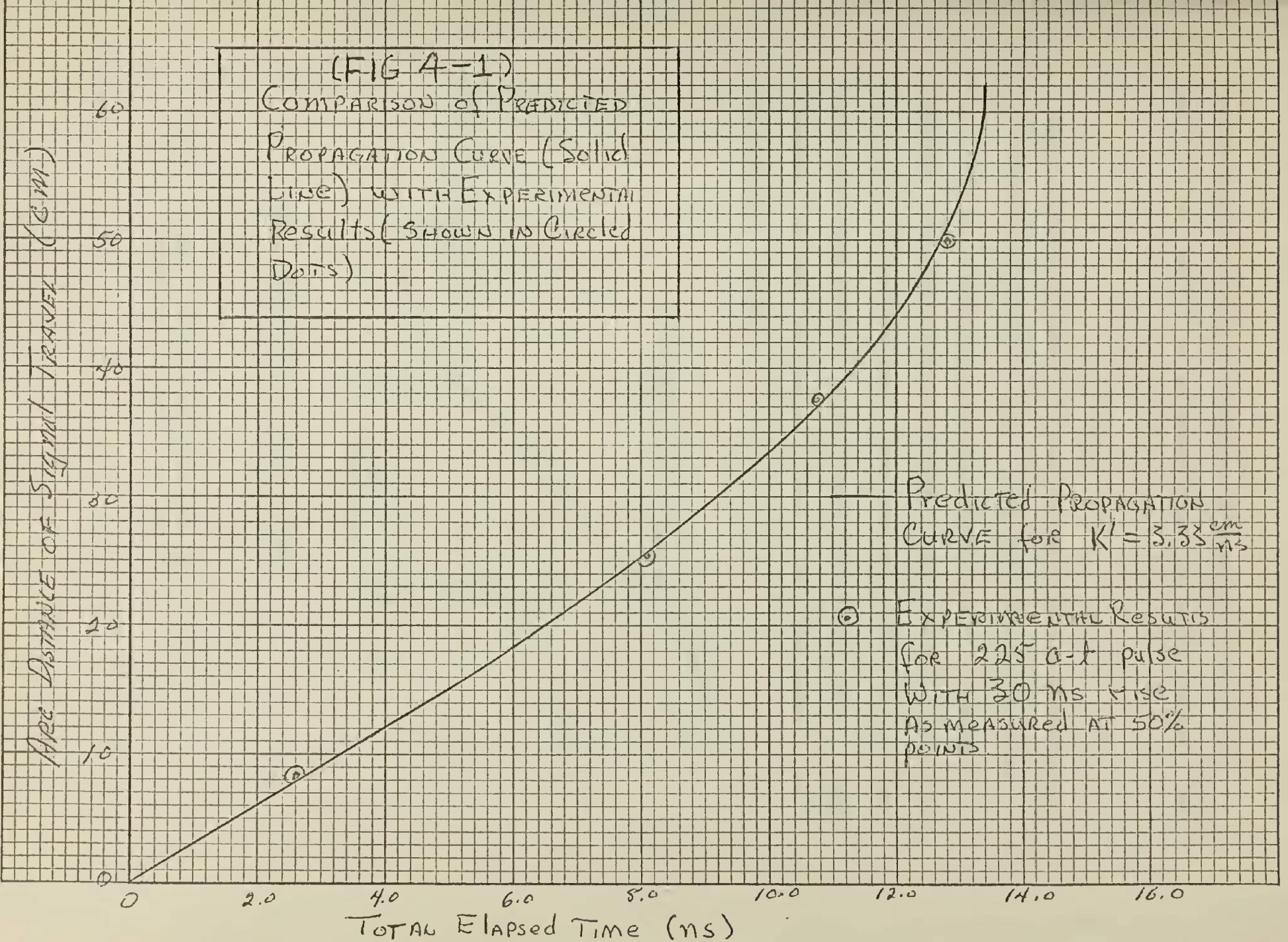

Then the apparent H critical (hereafter designated H') would be H reset plus the .085 $\frac{a\text{-}t}{cm}$ value obtained from the static hysteresis loop; or

$$H' = .285 \frac{a\text{-}t}{cm}$$

Next consider the factor K which corresponds to the slope of an applied ramp of magnetomotive force. From photo #4 and #5 showing respectively the 20 KV driving voltage wave form and the resulting current pulse, it is clear that a ramp function describes these pulse faces quite well. This is particularly true between the 10% to 90% of final value points which defines the rise time quoted in this thesis. Figure 4-2 presents the ramp idealization of the current pulse shown in photo #2 for the 225 a-t pulse.

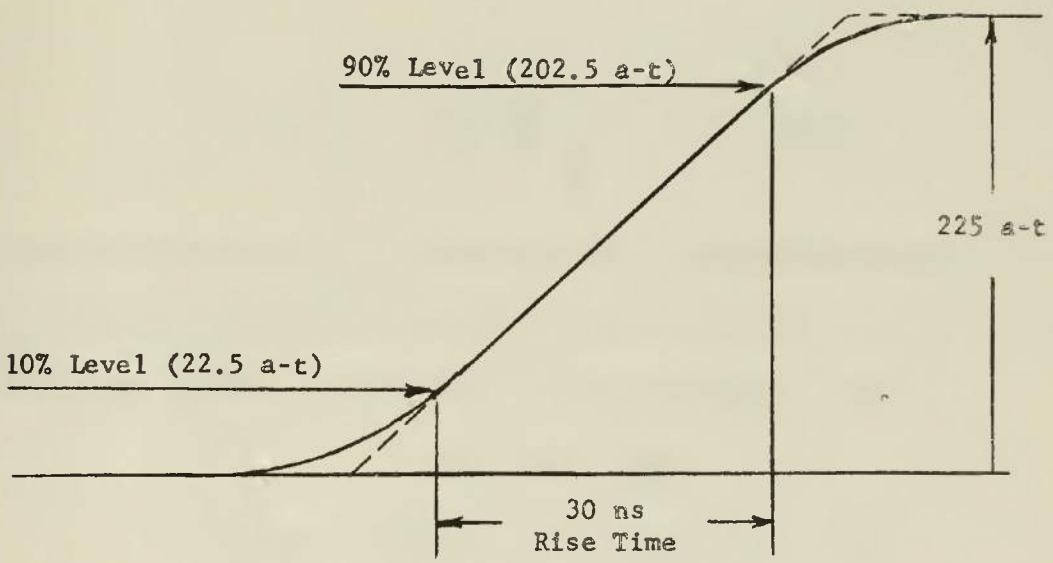

$$K = \frac{NI}{t} = \frac{202.5 - 22.5}{30} = \frac{180}{30} = 6.0 \frac{a\text{-}t}{ns}$$

Fig. 4-2 Ramp Function Idealization of MMF Pulse Rise for Calculation of slope constant, K.

As seen from the calculations accompanying the figure, K is dependent on the amplitude of the applied field. Hence, as we reduce the amplitude of this MMF pulse, the value of K will likewise be reduced. However, during the conduct of this experiment, H reset was reduced proportionately with the MMF magnitude in such a way as to just reset the core between pulses. This tends to affect the variation in K with the result that K' varies only slightly over the entire range of MMF pulses. Since K' fixes the apparent propagation rate, a corresponding small variation should be evident among the experimentally derived propagation curves. Such is indeed the case as can be observed from the graphs #1, #2, and #3 of Appendix I. To further illustrate these ideas, the value of K' for the 225 a-t pulse of MMF is found to be

$$K' = \frac{K}{2\pi H'} = \frac{6.0 \frac{\text{a-t}}{\text{ns}}}{2\pi(.285 \frac{\text{at}}{\text{cm}})} = 3.33 \frac{\text{cm}}{\text{ns}}$$

This is the value used in constructing the theoretical propagation curve shown in Figures 2-7 and 4-1. Now, if the 117 a-t pulse is analyzed in the same manner, a value of K' = 3.1 is obtained. That is

$$K = \frac{94}{30} = 3.13 \frac{\text{a-t}}{\text{ns}}$$

$$H \text{ reset} = \frac{10 \text{ a-t}}{125} = .08 \quad \text{hence } H' = .165$$

$$K = \frac{K}{2\pi H'} = 3.1 \frac{\text{cm}}{\text{ns}}$$

Thus, halving the MMF only reduces K' to a value 3.1 $\frac{\text{cm}}{\text{ns}}$. The curve for this value of K' is shown in Figure 4-3 along with the experimental data obtained for the 117 a-t pulse. Within experimental accuracy, the results are again quite good. However, it should be pointed out that above analysis

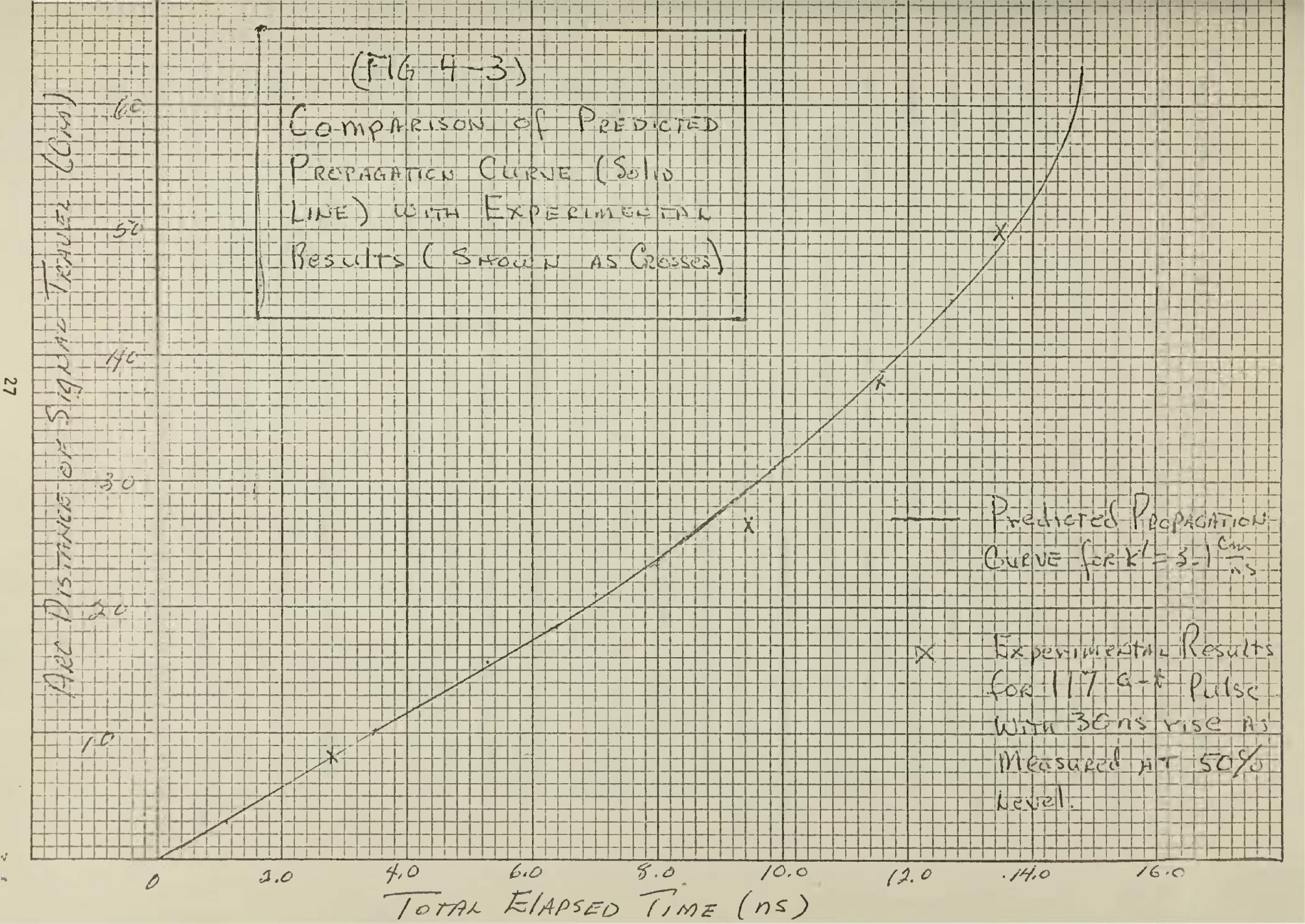
(FIG 4-3)
Comparison of Predicted Propagation Curve (Solid Line) with Experimental Results (Shown as Crosses)
Predicted Propagation Curve for K' = 3.1
Experimental Results for 117 G-L Pulse with 36 ns rise as Measured at 50% level.
Apex Distance or Signal Travel (cm)
Total Elapsed Time (ns)
10
20
30
40
50
60
0
2.0
4.0
6.0
8.0
10.0
12.0
14.0
16.0

has compared the predicted results with the experimental measurements taken for points on the pulse corresponding to 50% of the peak voltage. Comparison of Graphs #1 and #3 with Graph #2 (or an inspection of Graphs #4, #5, #6, and #7) reveals a moderate difference in the propagation curves plotted for 20% and 80% points as compared with the 50% curve. Certainly some of this difference results from experimental inaccuracies. However, a close examination of the current pulse shown in Photo #2 will shown that the pulse face is not a true ramp. The ramp approximation is at its best for the 50% points and less valid at the 20% and 80% levels.

In order to induce a significant change in K', the rise time of the applied MMF was varied as discussed in Chapter III. Since the final pulse magnitude remained unchanged for all of the various pulse rise times tested in this part of the experiment, the reset current remained unchanged. Hence H' remained constant and K' varied with changes in the pulse face slopes. Figure 4-4 is a comparison of the predicted curves with the actual experimental data for pulse rise times of 45 ns, 55 ns, and 75 ns and a pulse magnitude of 225 a-t. There is fair correlation between the predicted and measured propagation curves. Again, the data presented was for the 50% level and hence corresponds to that portion of the current pulse rise best suiting the assumption of a pure ramp function.

Before examining the third and final part of the experimental results, (that is apparent attenuation) the method used to convert the relative time recorded for the experimental data to the absolute time of the predicted propagation curve must be discussed. Recall that the delay time measured in the experiment was the relative time delay of the pickup

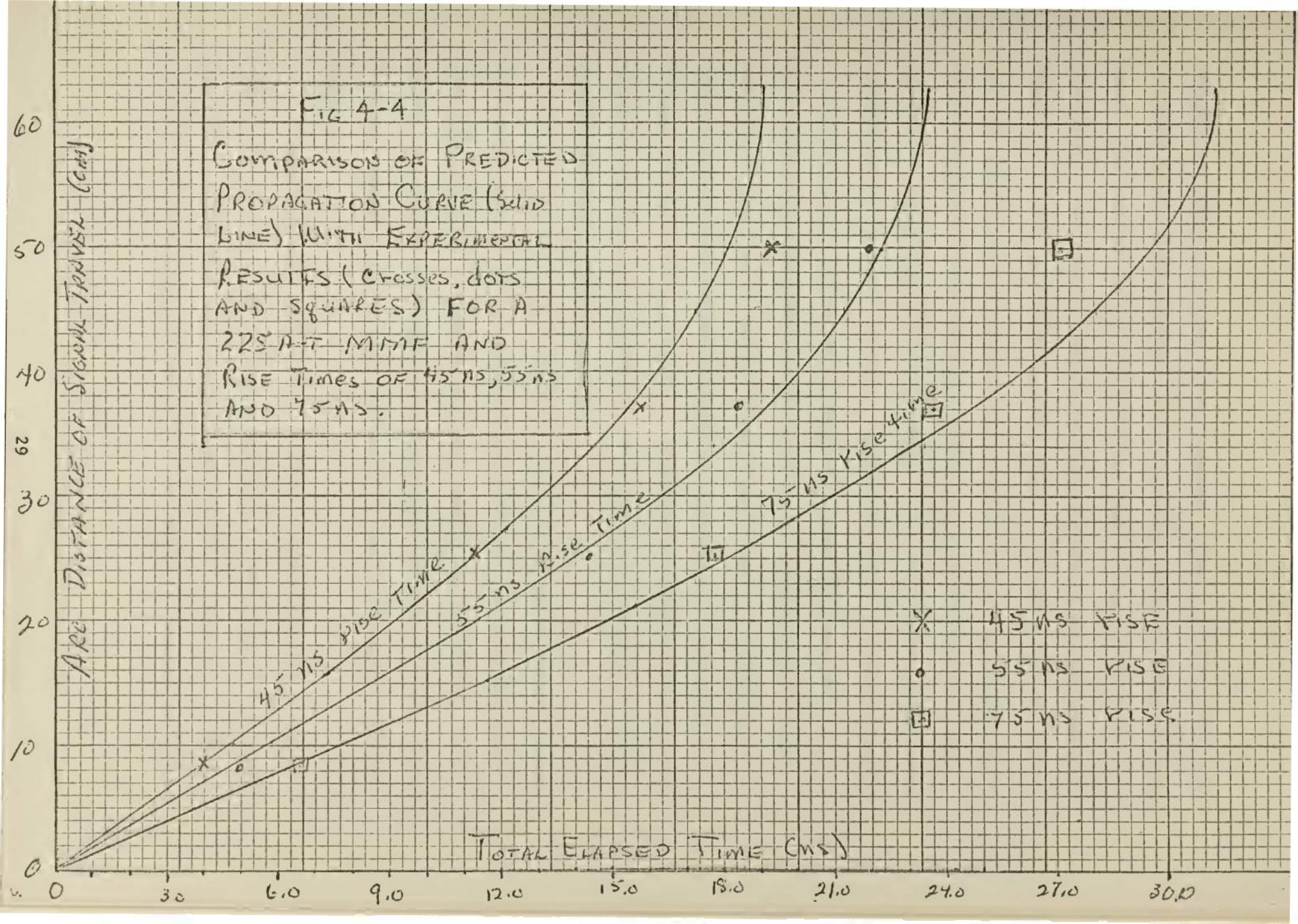
FIG 4-4
COMPARISON OF PREDICTED PROPAGATION CURVE (SOLID LINE) WITH EXPERIMENTAL RESULTS (CROSSES, DOTS AND SQUARES) FOR A 225 N-T MINE AND RISE TIMES OF 45 NS, 55 NS AND 75 NS.
ARC DISTANCE OF SIGNAL TRAVEL (CM)
TOTAL ELAPSED TIME (NS)
45 NS RISE TIME
55 NS RISE TIME
75 NS RISE TIME
X 45 NS RISE
o 55 NS RISE
75 NS RISE
0
10
20
30
40
50
60
0
3.0
6.0
9.0
12.0
15.0
18.0
21.0
24.0
27.0
30.0

signal with respect to some fixed reference signal. Therefore the plot of these delay times presents only the relative times of signal propagation. For example, to find the absolute time for the signal to travel from the 8.5 cm pickup to the 25.4 cm pickup will be the difference between the time delays of both pickup signals from the reference. To put the experimental data on the same time base as the predicted curves, it is necessary to shift the experimental time base linearly. This amounts to superimposing the experimental plot onto the predicted curve, neglecting the measured time base. Obviously there is a certain amount of curve fitting involved which may tend to make the experimental results coincide better than is really the case. However, the relative position of the plotted points of experimental data are fixed both by the position of the particular pickup on the core and by the time relation between the various points. Hence the only degree of freedom permitted in matching the predicted curve with the experimental one is a linear adjustment of the time base.

In a final test of the theory, a single winding was placed through the center of the core and excited with a 225 a-t pulse of MMF with a rise time of 30 ns. Since the exciting winding was equidistant from all points on the core, the magnetic field reached all points on the core at the same instant. This rather obvious experiment yielded the expected results.

Although the magnitude of the voltages appearing as the pickup signals is far too large to be the result of the MMF wave alone, a test was run to insure that these signals were actually the result of flux reversal within the magnetic material. The magnetic core was replaced

by a thin ring of stainless steel.* The exciting winding was then pulsed with 225 a-t MMF pulses with 30 ns rise time. The amplitude of the resulting pickup signals was less than 2% of the corresponding values obtained for the magnetic core. The signal to noise ratio was too high to permit collecting accurate data with the stainless steel configuration; however, the measurements taken yielded an average apparent velocity of approximately $2 \times 10^{10} \frac{cm}{sec}$. Within the accuracy possible with these small signals, this result conforms to that predicted in Figure 2-4.

One final element of the proposed theory remains to be discussed and that is the apparent attenuation of the induced signal with arc lergth of signal travel. In Chapter II, Figure 2-5 was constructed assuming the pulse amplitude decreased as the inverse of the chord length of travel. The magnitudes of the voltage spikes appearing on the pickup signals were measured and are plotted on Graph #9 of Appendix I. These curves were normalized with respect to a position on the core 10 cm from the exciting windings** and Graph #10 of Appendix I shows the resulting plot of these normalized curves. Assuming the voltage at a pickup is directly proportional to the MMF reaching that pickup (3) the normalized plot of Figure 2-5 and Graph #10 of Appendix I can be compared. Figure 4-5 shows the superposition of these two plots with the 10 cm ordinate intercept used as the common comparing point. It is evident that

*Stainless steel was used instead of copper since it is both non magnetic and has a conductivity approximately equal to that of 50% Ni-Fe.

**Normalization is necessary since a comparison is being made between a MMF and a resulting voltage.

the attenuation measured is somewhat greater than the predicted attenuation. This is certainly to be expected since initial nucleation of domains must consume a certain energy from the exciting pulse. This energy is permanently missing as a result of the ohmic losses resulting from microscopic eddy currents and anistotropic energy consumed in nucleation. (1)

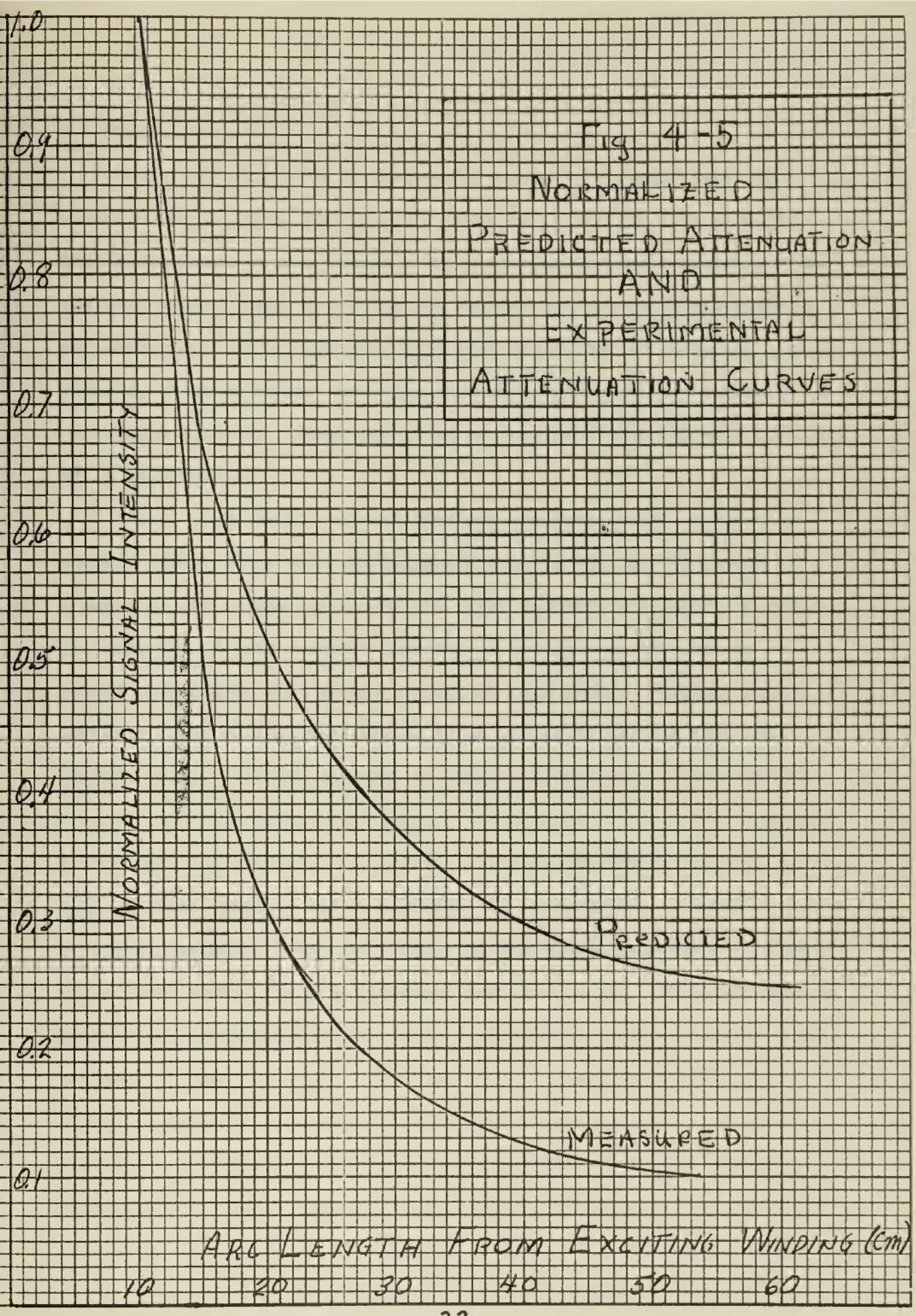

Fig 4-5
NORMALIZED
PREDICTED ATTENUATION
AND
EXPERIMENTAL
ATTENUATION CURVES

5. Conclusions

Certainly, no theory is adequately tested by a single experiment conducted by a single experimentor. Such is indeed the case with the theory developed in this thesis. While the implications resulting from the experimental data are strong and support the theoretical arguments, the theory must be tested under different conditions by different experimentors, using different measuring equipment and techniques before it can become accepted. What, then, can be concluded from the work presented in this thesis?

First, it is fairly evident that any circumferential propagation process taking place in a ferromagnetic torroid will be the result of a magnetic wave radiating across the inner diameter air space. Clearly, the velocity of such a signal transfer is far greater than can be expected from domain wall motion within the core tapes. Further, since magnetic lines of flux must always close on themselves and link the current in the exciting winding, it becomes impossible to establish an H field about the entire core without the magnetic field first sweeping across the inner diameter air space. The proposed theory complies with both of these concepts and in addition, it is certainly a possible method of signal transfer. When the results of the simple experiment of Chapter II are considered, the theory becomes more convincing. Obviously energy cannot be transferred about the core circumference with a velocity greater than the speed of light. Yet, there is the undeniable evidence in Graphs 1 through 8 of Appendix I which shows this velocity to approach infinity. This seeming paradox is readily explained by the proposed theory and is, indeed, one of its fundamental characteristics. Further,

the reasonable predictability of apparent circumferential propagation velocity using simple trigonometric methods offers strong support to the argument. In view of these facts, it is concluded that the circumferential propagation process takes place by means of an E-M energy transfer directly from the source of MMF to the nucleation sites about the core. Subsequent energy is also transferred by this radiation process with the final result being a growth of the domains of reversed magnetization and radial domain wall motion.

APPENDIX I

PLOTS OF EXPERIMENTAL DATA

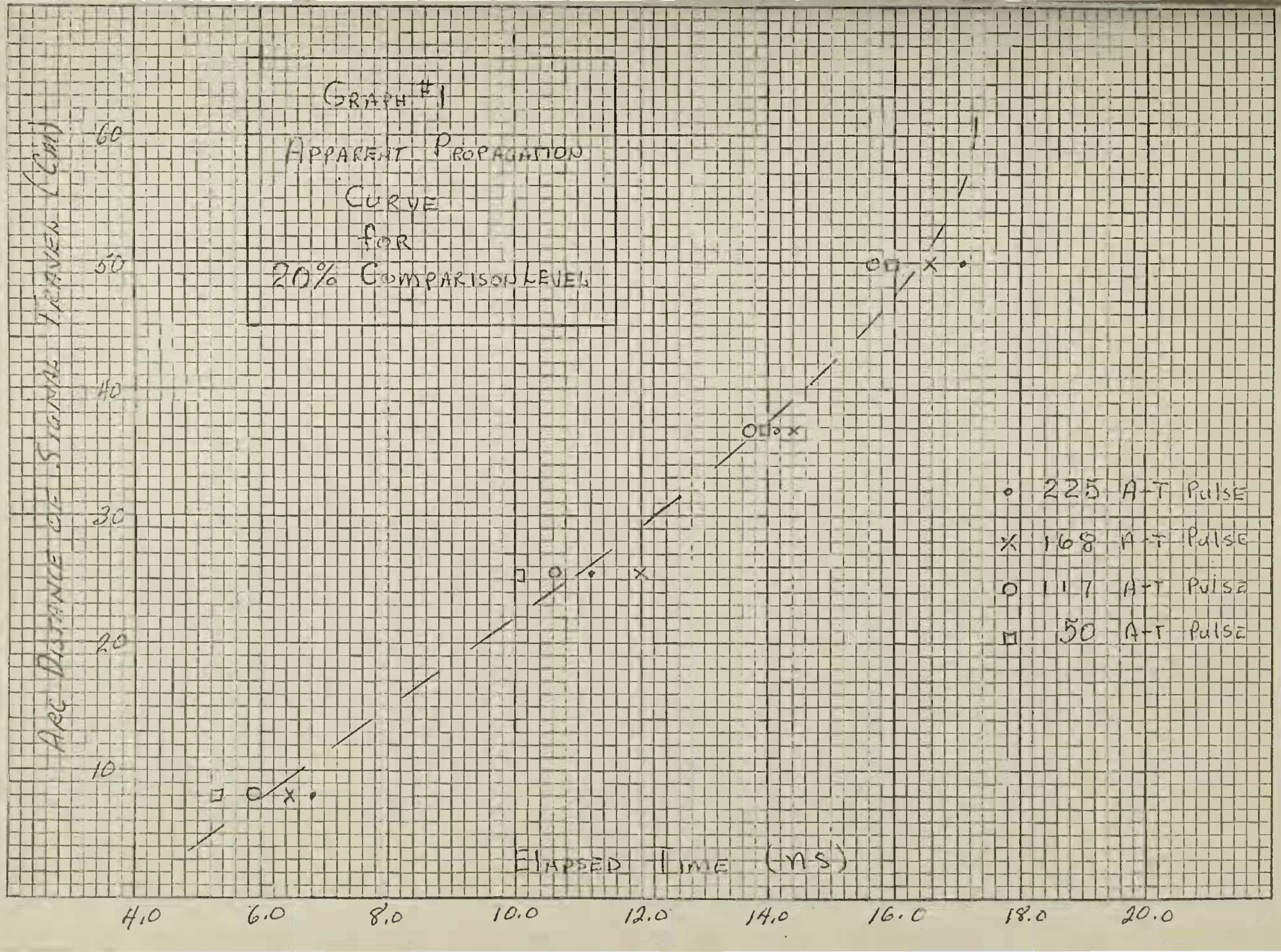
GRAPH #1
APPARENT PROPAGATION
CURVE
FOR
20% COMPARISON LEVEL
ARC DISTANCE OF SIGNAL TRAVEL (KM)
60
50
40
30
20
10
ELAPSED TIME (MS)
4.0
6.0
8.0
10.0
12.0
14.0
16.0
18.0
20.0
• 225 A-T Pulse
× 168 A-T Pulse
○ 117 A-T Pulse
□ 50 A-T Pulse

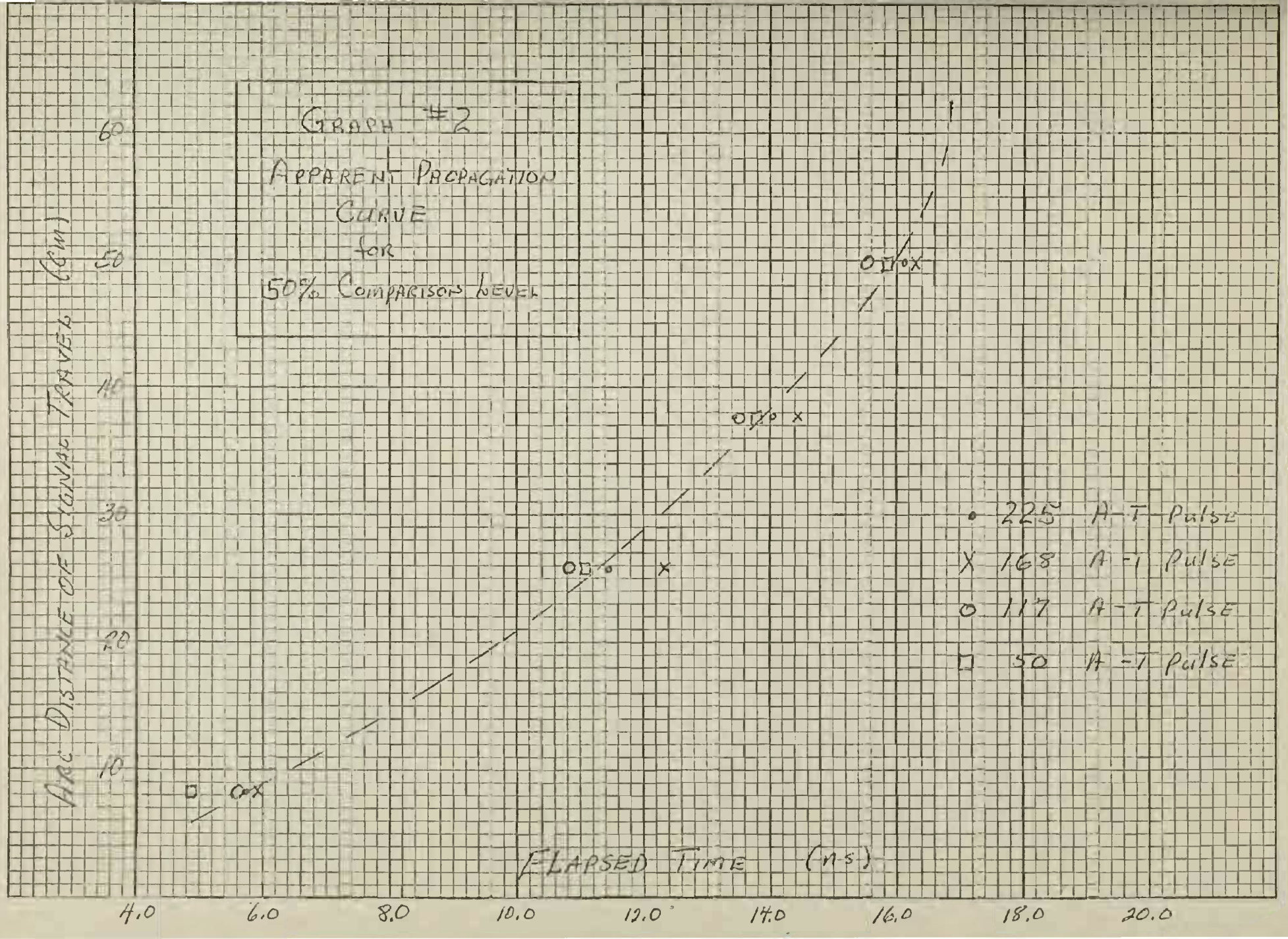
GRAPH #2
APPARENT PROPAGATION CURVE
for
50% COMPARISON LEVEL
ARC DISTANCE OF SIGNAL TRAVEL (CM)
60
50
40
30
20
10
4.0
6.0
8.0
10.0
12.0
14.0
16.0
18.0
20.0
ELAPSED TIME (NS)
• 225 A-T Pulse
X 168 A-T Pulse
○ 117 A-T Pulse
□ 50 A-T Pulse

GRAPH # 3

APPARENT PROPAGATION CURVE FOR 80% COMPARISON LEVEL

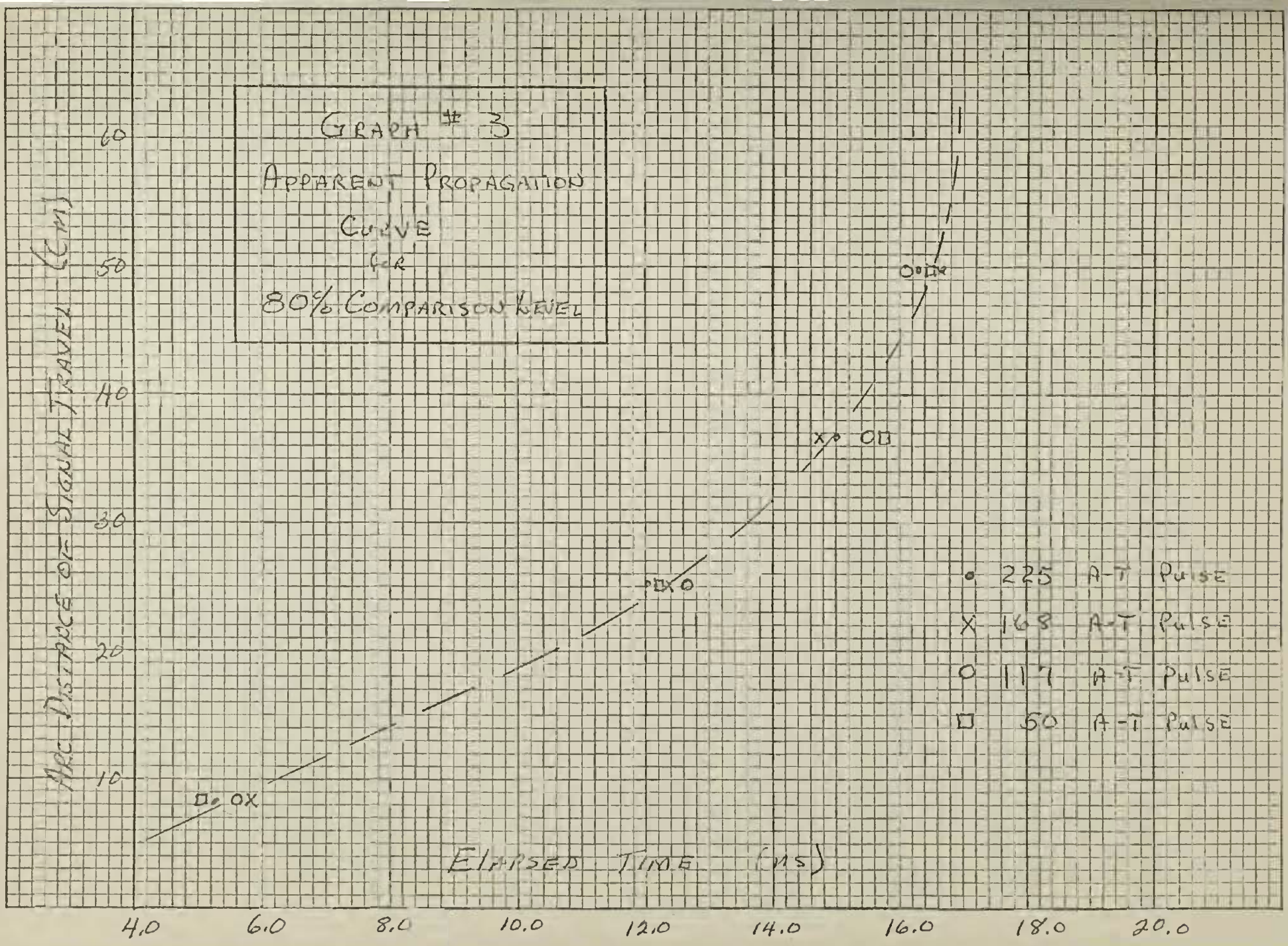

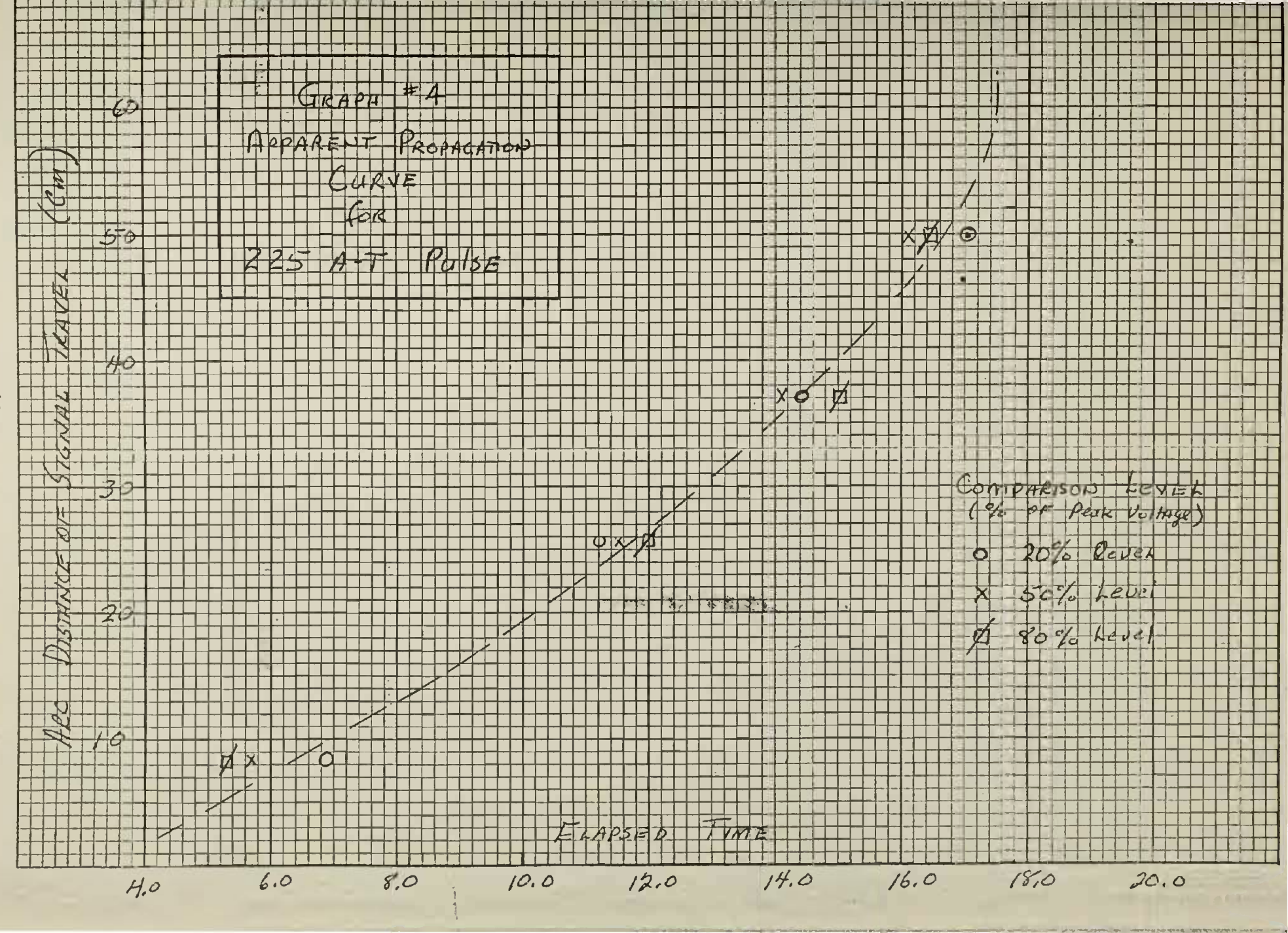
GRAPH #4
APPARENT PROPAGATION CURVE FOR 225 A-T PULSE
ABS. DISTANCE OF SIGNAL TRAVEL (cm)
60
50
40
30
20
10
ELAPSED TIME
4.0
6.0
8.0
10.0
12.0
14.0
16.0
18.0
20.0
COMPARISON LEVEL (% of Peak Voltage)
○ 20% Level
× 50% Level
Ø 80% Level

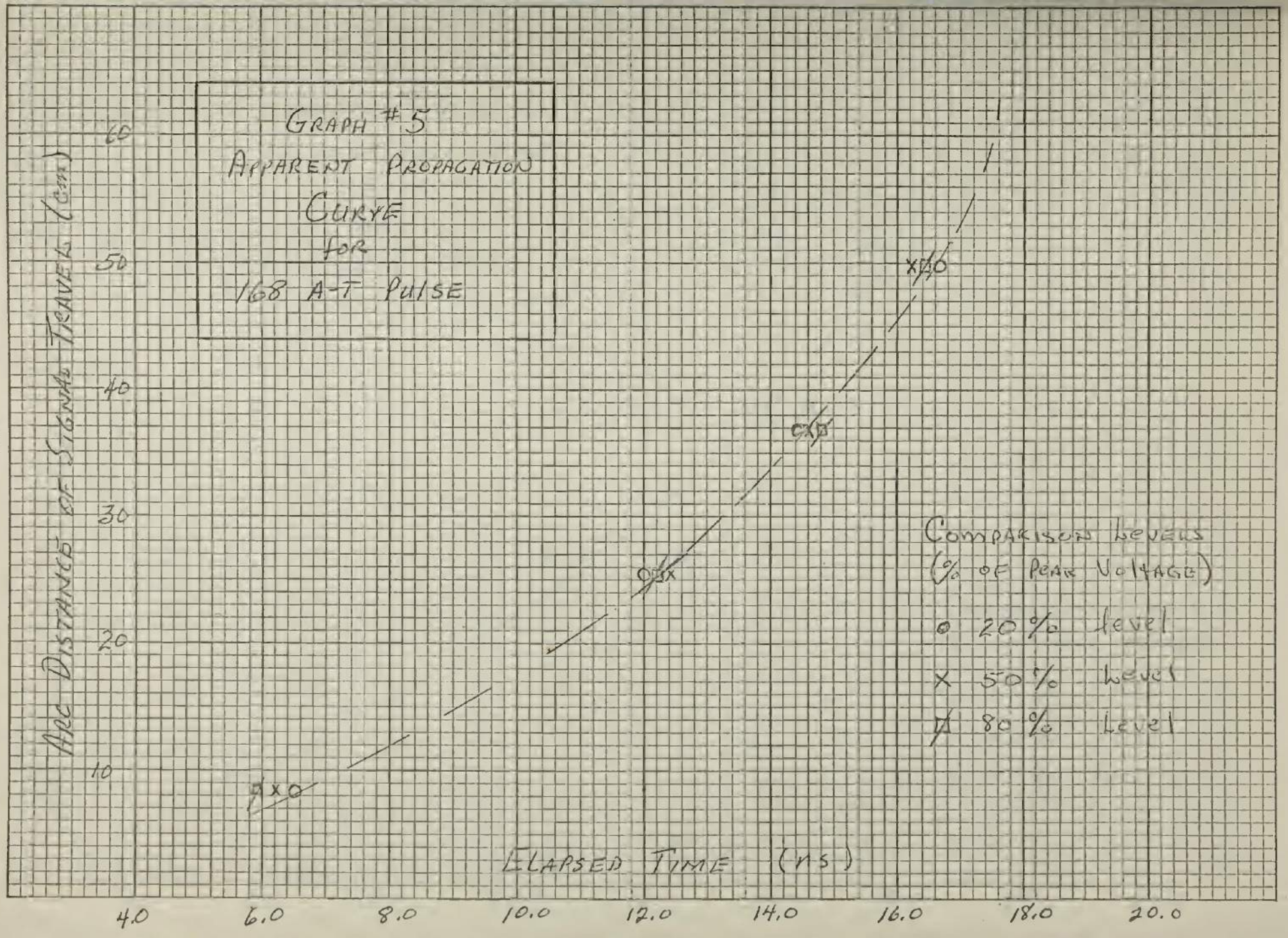
GRAPH #5
APPARENT PROPAGATION
CURVE
FOR
168 A-T PULSE
ARC DISTANCE OF SIGNAL TRAVELS (CMS)
ELAPSED TIME (NS)
10
20
30
40
50
60
4.0
6.0
8.0
10.0
12.0
14.0
16.0
18.0
20.0
COMPARISON LEVELS
(% OF PEAK VOLTAGE)
○ 20% level
× 50% level
□ 80% level

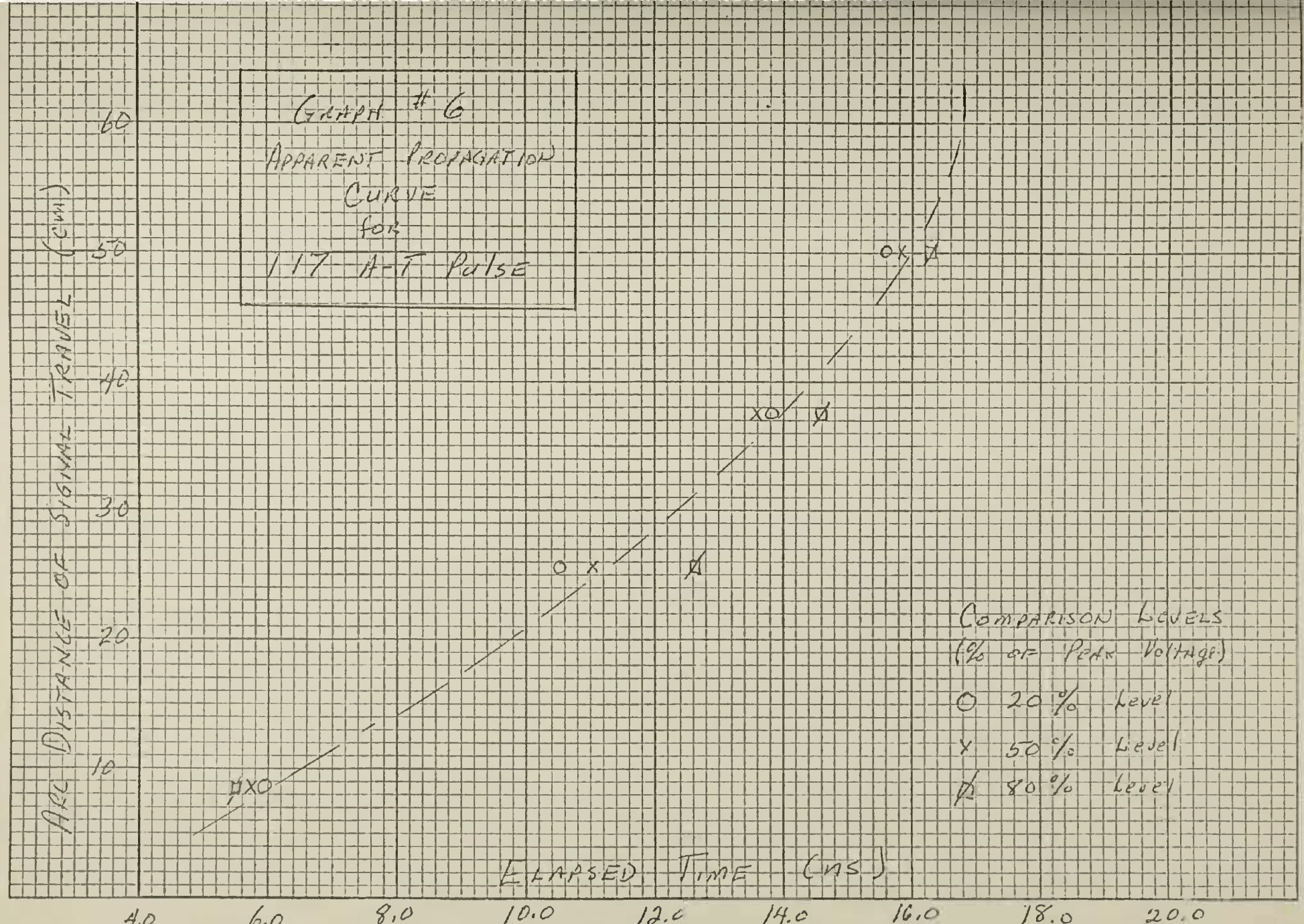
GRAPH #6
APPARENT PROPAGATION CURVE
for
117 A-T Pulse
ARC DISTANCE OF SIGNAL TRAVEL (cm)
60
50
40
30
20
10
ELAPSED TIME (ns)
4.0
6.0
8.0
10.0
12.0
14.0
16.0
18.0
20.0
COMPARISON LEVELS
(% of Peak Voltage)
○ 20 % Level
× 50 % Level
∅ 80 % Level

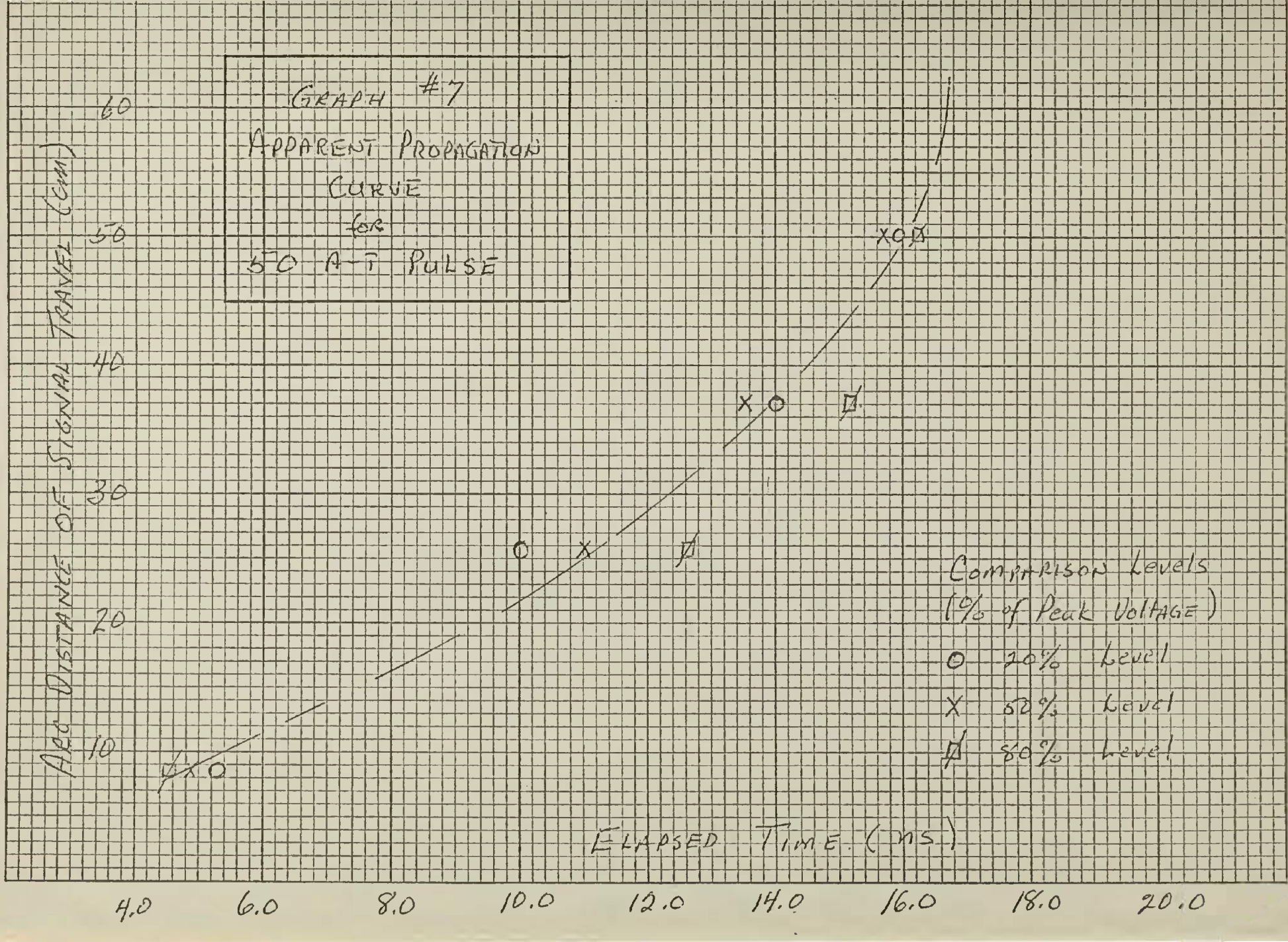
GRAPH #7
APPARENT PROPAGATION CURVE
for
50 A-T PULSE
APP. DISTANCE OF SIGNAL TRAVEL (cm)
60
50
40
30
20
10
ELAPSED TIME (ns)
4.0
6.0
8.0
10.0
12.0
14.0
16.0
18.0
20.0
Comparison Levels
(% of Peak Voltage)
20% Level
50% Level
80% Level

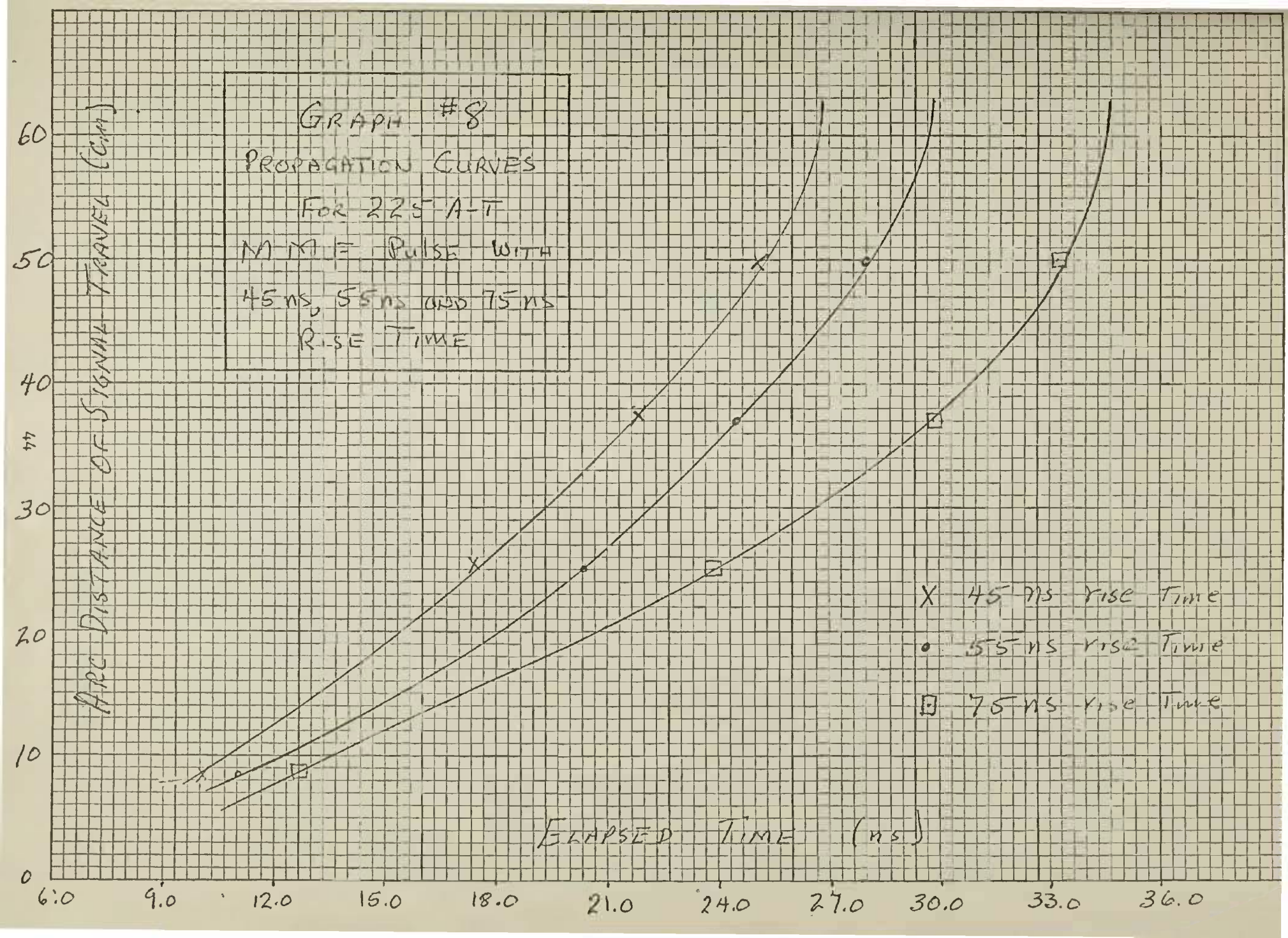
GRAPH #8
PROPAGATION CURVES
FOR 22 S A-T
MMF PULSE WITH
45 ns, 55 ns AND 75 ns
RISE TIME
ARC DISTANCE OF SIGNAL TRAVEL (cm)
ELAPSED TIME (ns)
X 45 ns Rise Time
• 55 ns Rise Time
□ 75 ns Rise Time
0
10
20
30
40
50
60
6.0
9.0
12.0
15.0
18.0
21.0
24.0
27.0
30.0
33.0
36.0

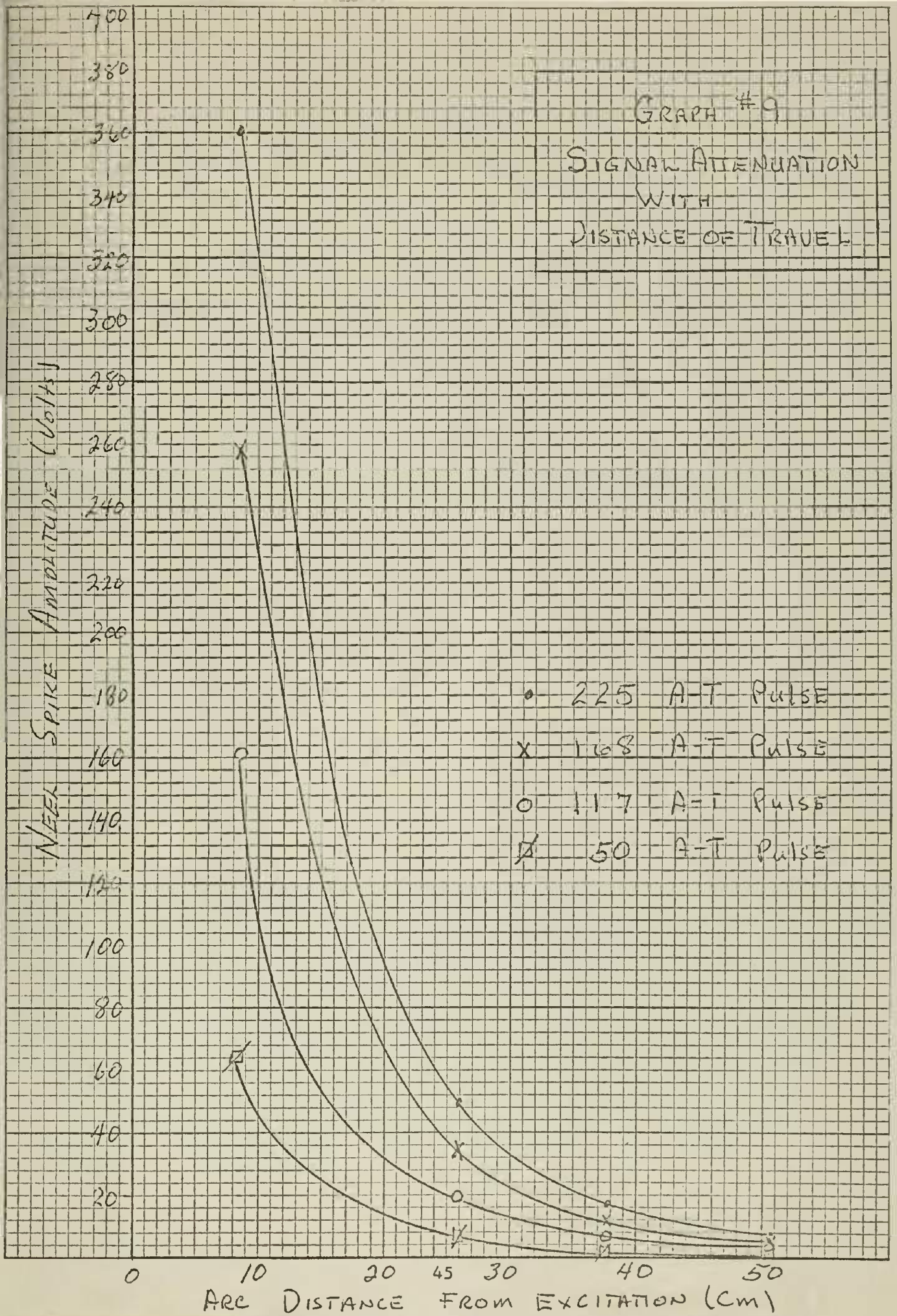
GRAPH #9
SIGNAL ATTENUATION
WITH
DISTANCE OF TRAVEL
NEG. SPIKE AMPLITUDE (VOLTS)
400
380
360
340
320
300
280
260
240
220
200
180
160
140
120
100
80
60
40
20
• 225 A-T PULSE
X 168 A-T PULSE
O 117 A-T PULSE
Ø 50 A-T PULSE
0
10
20
45
30
40
50
ARC DISTANCE FROM EXCITATION (Cm)

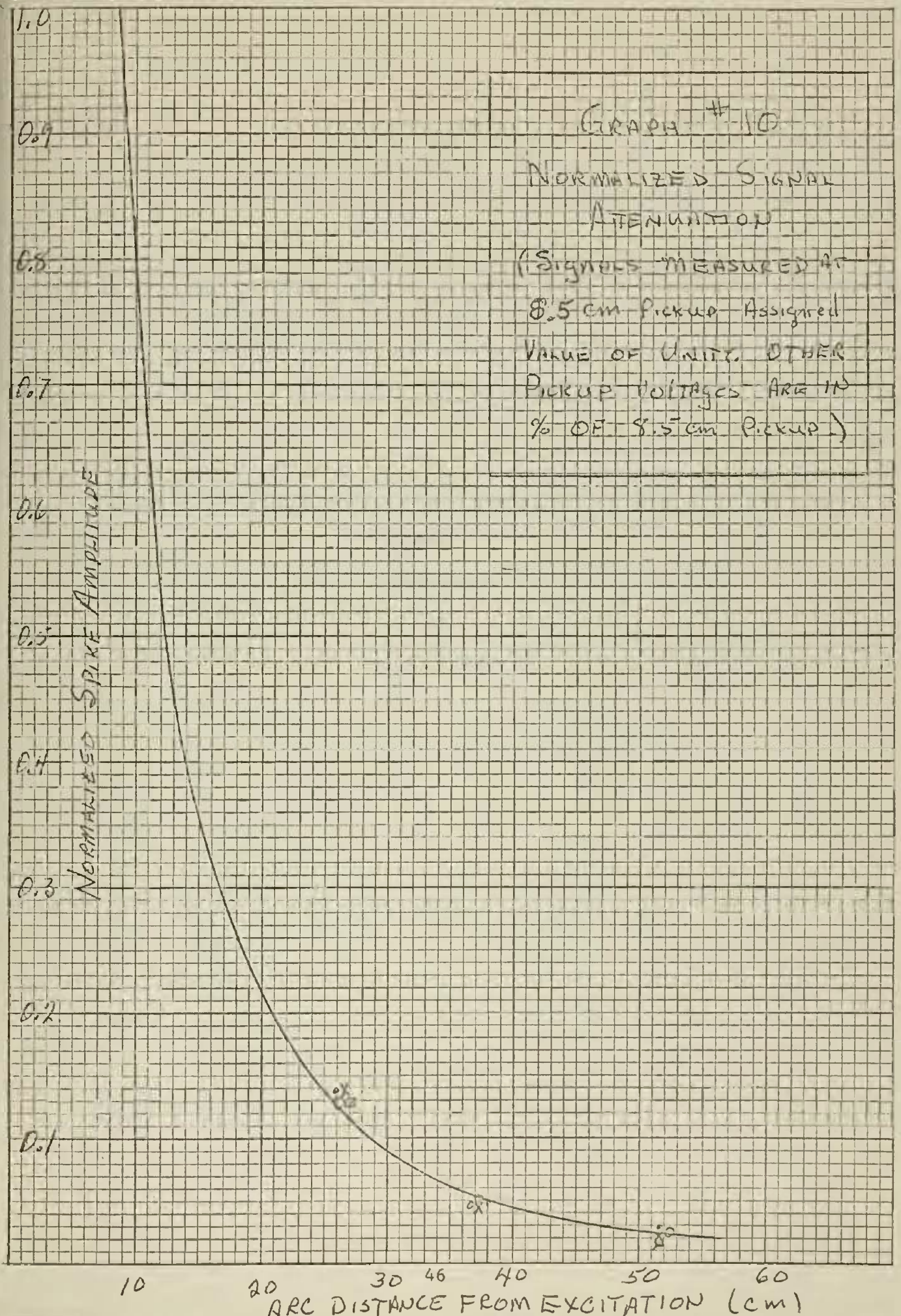
GRAPH # 10
NORMALIZED SIGNAL ATTENUATION
(SIGNALS MEASURED AT 8.5 cm PICKUP ASSIGNED VALUE OF UNITY. OTHER PICKUP VOLTAGES ARE IN % OF 8.5 cm PICKUP)
NORMALIZED SPIKE AMPLITUDE
1.0
0.9
0.8
0.7
0.6
0.5
0.4
0.3
0.2
0.1
10
20
30
46
40
50
60
ARC DISTANCE FROM EXCITATION (cm)

APPENDIX II

PHOTOGRAPHS

OF

PULSE SHAPES

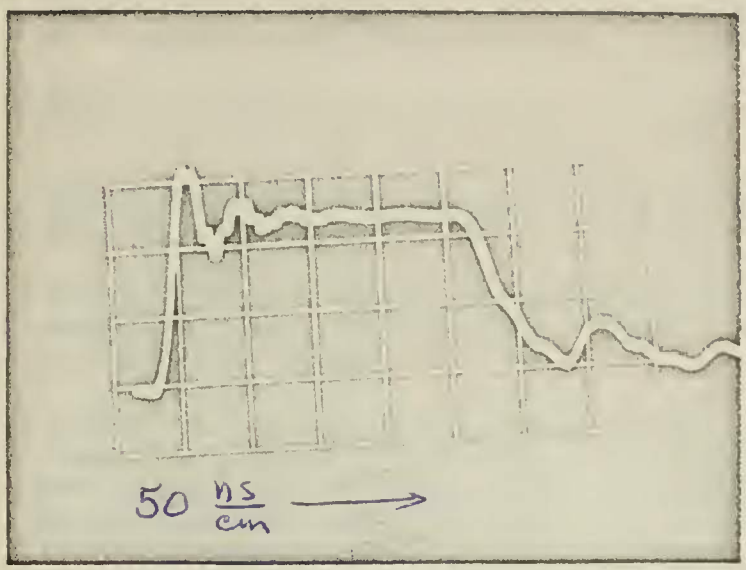

PHOTO #1

20KV DRIVING VOLTAGE PULSE

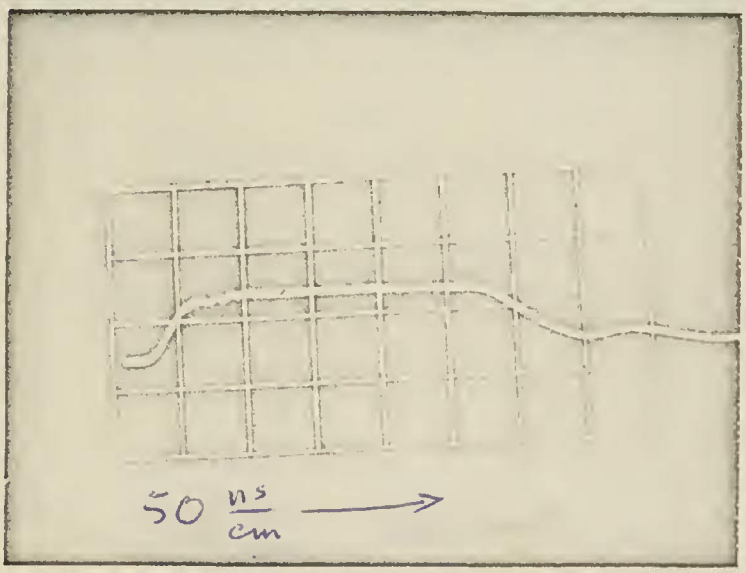

PHOTO #2

225 A-T CURRENT PULSE

BIBLIOGRAPHY

1. Magnetization in Tape-Wound Cores, R. C. Barker, AIEE Transactions Pt I, Communication and Electronics, Vol. 80 pp 482-503.

2. Solid State Magnetic and Dielectric Devices, (book), H. W. Katz, John Wiley and Sons, Inc., New York, 1959.

3. Fields and Waves in Modern Radio, (book) Simon Ramo and J. R. Whinnery, John Wiley and Sons, Inc., New York, Second Edition, 1953.

4. Theory of Domain Creation and Coercive Force in Polycrystalline Ferromagnetics, J. B. Goodenough. Physical Review, Vol. 95, no. 4, Aug. 1954, pp. 917-32.

5. Superposed Magnetization in Materials with Rectangular Hysteresis Loops, C. B. Wakeman. Doctoral Dissertation, Yale University, New Haven, Conn., May 1955; also Technical Report 56-199 Wright Air Development Center, Dayton, Ohio, Pt. II, also available, No. PB 131209, Department of Commerce, Washington, D. C.

6. Flux Reversal in Magnetic Amplifier Cores, F. J. Friedlander, AIEE Transactions, Pt. I (Communication and Electronics), Vol. 75, July 1956, pp. 268-78.

7. Propagation of Large Barkhausen Discontinuities, K. J. Sixtus, L. Touks. Physical Review, New York, N. Y., Vol. 43, 1933, pp. 931-40.

8. Introduction to Solid State Physics, (book), Charles Kittel, John Wiley and Sons, Inc., New York, Second Edition, 1956.